

POLITECNICO DI TORINO

Master Degree in Biomedical Engineering

Master Degree Thesis

**Artifacts removal and application
of cross-frequency coupling to
EEG signals of epileptic patients**



Supervisor
Prof. Luca Mesin

Candidate
Giulia MACAUDA

December 2020

*Alla mia famiglia che
ha sempre creduto in
me*

Abstract

Epilepsy is a neurological condition characterized by recurrent episodes, called convulsive seizures, consisting of sudden and repeated muscle movements, often associated with temporary suspension of the state of consciousness. Seizures are generally of very short duration, although they can sometimes last for a long time, and are the result of an abnormal and prolonged synchronization of the activity of neurons in the cerebral cortex or brainstem. Through the use of an innovative approach, such as the association of EEG and functional magnetic resonance imaging, EEG-fMRI, it is possible to map the specific functional activation of certain brain areas.

In particular, this thesis focuses on the study of the interaction between oscillations at different frequency bands. This is called cross-frequency coupling, CFC. The CFC analyses the mechanisms that regulate neuronal processing distributed between the various brain frequencies. This integration of the processing between frequencies could be obtained through the CFC, specifically the phase-amplitude coupling, PAC.

Before studying CFC in our data, it was essential to proceed with the cleaning of signals from artifacts. Indeed artifacts, such as eye movements, blinking, heart signals, muscle noise, and power line interference present serious problems for the EEG interpretation and analysis. To remove artifacts from EEG recordings, especially those resulting from eye movements and blinking, many methods have been developed. In particular, in this thesis, the analysis of independent components for the removal of artifacts has been analysed and applied.

Once the data has been cleaned, cross-frequency coupling was investigated before and after eye closing in patients with eyelids myoclonia with absences, a rare epilepsy syndrome with seizures evocated by eye closure plus seizures that appear spontaneously. Typically, seizures occur within 3 seconds after eye closure. The data were also collected in a rest condition, i.e. the situation where a subject does not perform any specific task.

Ringraziamenti

Prima di procedere con la trattazione, vorrei dedicare qualche riga a tutti coloro che mi sono stati vicini in questo percorso di crescita personale e professionale.

Ringrazio il Prof. Luca Mesin per l'aiuto che mi ha fornito e per la disponibilità durante tutto questo periodo. Mi ha accompagnato in questi mesi con preziosi consigli che mi hanno permesso di concludere al meglio questo percorso.

Un ringraziamento va alla Dott.ssa Vaudano e alla Dott.ssa Talami per avermi trasmesso la passione per il vostro lavoro permettendomi di approfondire molte tematiche interessanti.

Un immenso grazie va a mia mamma, la quale mi ha sempre sostenuto e ha costantemente creduto in me. Senza tutto ciò che hai fatto non sarebbe stato possibile raggiungere questo mio traguardo. Grazie per avermi insegnato tutti i valori che mi hanno permesso di diventare la donna che sono oggi.

Un ringraziamento speciale va a Daniele. A te che mi hai sopportato, sopportato, spronato e incoraggiato a dare sempre il meglio. Abbiamo condiviso questo cammino, passo dopo passo, superando tutte le difficoltà, festeggiando insieme ogni vittoria e rialzandoci più forti dopo ogni sconfitta.

Grazie a mia nonna Rachele per l'affetto che non mi ha mai fatto mancare e per essere sempre stata orgogliosa di me.

Vorrei ringraziare tutta la mia famiglia. Il vostro sostegno e amore dimostratomi ogni giorno, è stato fondamentale per addolcire questi anni. E' anche grazie al vostro incoraggiamento se sono riuscita a raggiungere questo obiettivo.

Ringrazio Valeria, presenza costante in questi anni, Anna, Matteo, Simona, Carla, Nicole e a tutti quelli che per un periodo più o meno lungo mi son stati vicini condividendo paure e gioie. Grazie a voi per aver allietato questi anni.

Un ultimo ringraziamento va a me stessa per non aver mai mollato anche quando sembrava sempre più difficile, per la determinazione e l'impegno attuo a raggiungere questo traguardo.

Contents

Acronyms	VIII
List of Figures	IX
List of Tables	XI
1 Introduction	1
1.1 Thesis Motivation	1
1.2 Thesis Structure	2
2 Electroencephalographic signal and Epilepsy	4
2.1 Nervous System	5
2.2 Central Nervous System	5
2.2.1 Cells of CNS	6
2.2.2 Synapse	8
2.3 The human brain	10
2.3.1 Cerebral cortex and functional areas	11
2.4 EEG	13
2.4.1 Feature	14
2.4.2 Frequency bands	14
2.5 The International 10-20 System of Electrode Placement	17
2.6 Functional Magnetic Resonance - fMRI	19
2.6.1 EEG-fMRI	21
2.7 Epilepsy	22
2.7.1 Classification	22
2.7.2 Therapy	24
3 Independent Component Analysis to remove EEG's artifacts	25
3.1 Artifacts	25
3.1.1 Types of artifacts	25
3.2 Blind Sources Separation	28
3.2.1 Definition	29

3.3	Independent Component Analysis	30
3.3.1	Assumptions	30
3.3.2	Pre-processing for ICA	31
3.3.3	Measurement of non-gaussainity	32
3.3.4	Limitations and advantages of ICA	35
3.4	ICA Decomposition	36
3.4.1	Decomposition algorithms	37
4	Cross-frequency coupling	38
4.1	Feature extraction steps	39
4.1.1	Band component extractions	39
4.1.2	Phase and amplitude extraction	40
4.2	Coupling Indexes	40
4.3	CFC and Neural Disorder	42
5	Results and Discussions	44
5.1	Dataset	44
5.1.1	Eyelid myoclonia with absences	46
5.2	Ocular Artifact Removal	47
5.3	Cross-frequency coupling	50
5.3.1	Phase Locking Value - PLV	51
5.3.2	Phase Amplitude Coupling - PAC	57
6	Conclusion	64
6.1	Future Work	64
6.1.1	Functional Connectivity	65
	References	67

Acronyms

AED	Anti-Epileptic Drug.
BOLD	Blood Oxygenation Level Dependent.
BSS	Blind Sources Separation.
CFC	Cross-Frequency Coupling.
CNS	Central Nervous System.
CSF	CerebroSpinal Fluid.
ECG	Electrocargiography.
EEG	Electroencephalography.
EMA	Eyelid Myoclonia with Absences.
EMG	Electromyography.
EOG	Electrooculography.
FD	Fractal Dimension.
FIR	Finite Impulsive Response.
FIR	Infinite Impulsive Response.
fMRI	functional Magnetic Resonance Imaging.
ICA	Independent Component Analysis.
ILAE	International League Against Epilepsy.
MI	Modulation Index.
MVL	Mean Vector Length.
PAC	Phase-Amplitude Coupling.
PLV	Phase Locking Value.
PNS	Peripheral Nervous System.
SNR	Signal to Noise Ratio.

List of Figures

2.1	<i>Structure of neurons</i>	6
2.2	<i>CNS cells: interaction between neurons and neuroglia</i>	8
2.3	<i>Functional anatomy of a chemical synapse (on the left) and an electrical synapse (on the right)</i>	9
2.4	<i>The encephalon. A) Lateral view of the encephalon, brainstem and cerebellum are shown. B) Anterior view of the encephalon: it is possible to observe the two emispheres and the longitudinal fissure</i> .	10
2.5	<i>Lobes of the cerebrum. This lateral view of the left cerebrum shows its four distinct lobes: frontal, parietal, occipital, and temporal</i> . . .	12
2.6	<i>Example of Delta wave</i>	15
2.7	<i>Example of Theta wave</i>	15
2.8	<i>Example of Alpha wave</i>	16
2.9	<i>Example of Beta wave</i>	17
2.10	<i>Example of Gamma wave</i>	17
2.11	<i>Electrode placement system according to the international standard</i> .	18
2.12	<i>Example of monopolar (left) and bipolar (right) derivation</i>	19
2.13	<i>Integration of EEG and fMRI technique</i>	21
3.1	<i>Waveform of some of the most common artifacts in EEG's signal</i> .	26
3.2	<i>The cocktail party problem</i>	28
3.3	<i>Gaussian, sub-gaussian and super-gaussian distributions</i>	33
3.4	<i>Component Properties for a single IC in EEGLAB</i>	36
5.1	<i>Example of an EEG plotting</i>	48
5.2	<i>Extract of an epoch 20s long before removal of the eye artifact</i> . . .	49
5.3	<i>The same epoch after removal of the eye artifact</i>	49
5.4	<i>Representation of the 10 most paired electrodes in the delta rhythm divided in the five cases of clinical interest</i>	52
5.5	<i>Representation of the 10 most paired electrodes in the theta rhythm divided in the five cases of clinical interest</i>	53
5.6	<i>Representation of the 10 most paired electrodes in the alpha rhythm divided in the five cases of clinical interest</i>	54

5.7	<i>Representation of the 10 most paired electrodes in the beta rhythm divided in the five cases of clinical interest</i>	55
5.8	<i>Representation of the 10 most paired electrodes in the gamma rhythm divided in the five cases of clinical interest</i>	56
5.9	<i>Representation of the heatmap to illustrate the PAC of the theta rhythm divided in the five cases of clinical interest</i>	58
5.10	<i>Representation of the heatmap to illustrate the PAC of the alpha rhythm divided in the five cases of clinical interest</i>	59
5.11	<i>Representation of the heatmap to illustrate the PAC of the beta rhythm divided in the five cases of clinical interest</i>	60
5.12	<i>Representation of the heatmap to illustrate the PAC of the gamma rhythm divided in the five cases of clinical interest</i>	61
5.13	<i>Representation of the heatmap to illustrate the PAC of the coupling between alpha and gamma rhythms divided in the five cases of clinical interest</i>	62
5.14	<i>Representation of the heatmap to illustrate the PAC of the coupling between theta and beta rhythms divided in the five cases of clinical interest</i>	63
6.1	<i>Overview of the main functional connectivity survey groups.</i>	66

List of Tables

2.1	EEG signal rhythms	15
5.1	Demographic and Eletroclinical Features of Patients with EMA . .	45

Chapter 1

Introduction

1.1 Thesis Motivation

The aim of this thesis is the study of cross-frequency coupling in epileptic patients. The study of CFC, cross-frequency coupling, has been linked to many brain functions and dysfunctions, including epilepsy. Epilepsy is a neurological condition characterised by recurrent seizures, defined as a sudden paroxysmal synchronous abnormal discharge of neuronal activity. In particular, eyelid myoclonia with absences, EMA, is an epileptic syndrome characterised by EEG paroxysms and photosensitivity induced by eye closure. In this thesis, we studied CFC from the EEG data of 15 EMA patients.

Before beginning with the study of CFC, it was essential to cleanse the signals from artifact. Indeed, artifacts such as eye movements, blinking, heart signals, muscle noise and power line interference present serious problems for the interpretation and analysis of EEG. Many methods have been developed in the literature to remove artifacts from EEG recordings, especially those resulting from eye movements and blinking. In particular, in this thesis, the analysis of independent components for the removal of these artifacts has been analysed and applied.

Once the data were cleaned, cross-frequency coupling was studied. For the study, 6-second epochs centred at the exact moment of eye closure were considered. There was a comparison between cases where the patient had or had not had an epileptic seizure following closure of the eye. In particular for the calculation of CFC it is possible to calculate different couplings, but the one elaborated in this thesis is the PAC, i.e. the phase-width coupling. Two different bands characterising the EEG signal, the low frequency phase of the alpha oscillation and the high frequency amplitude in the gamma band, were considered for the study.

1.2 Thesis Structure

After a careful study of the literature to better understand the physiology and determinant characteristics of the EEG signal, in the initial part of my thesis work I focused on the application and study of independent component analysis, ICA. This is a particular technique used extensively for the removal of artifacts, both physiological and extra-physiological. In particular, this thesis was aimed at removing the eye blink. Through studies of various works in the literature, ICA allows a large number of parameters to be set in order to obtain the desired results. To do this, several packages and toolboxes were tested before deciding which was the best for our specific data. Once the most effective method was selected for us, all EEG signals were cleared of artifacts.

Subsequently, the thesis work continued with the study of cross-frequency coupling. In fact, it emerged that the oscillations at the different frequencies that make up the brain rhythms are not isolated and independent. Instead, they work in a unified way and interact with each other. A correct interaction between the different oscillations is synonymous of a correct functioning of the brain activity, on the contrary an incorrect coupling can be synonymous of different pathologies.

The thesis is developed in the following chapters:

- In the second chapter the EEG signal is introduced, with an in-depth description of its physiological nature and how it is acquired. There is an introduction part with its main features and the waveforms that characterise this signal illustrated and described. A mention is also made of epilepsy, being the studied dataset of epileptic patients. Epilepsy is a disease of the central nervous system in which the activity of nerve cells in the brain is interrupted causing convulsions, periods of unusual behaviour and sometimes loss of consciousness.
- In the third chapter of the thesis there is an overview of the various artifacts that corrupt EEG signals. In fact, the EEG signal is largely corrupted by artifacts of different kinds, both physiological and extra-physiological. In the first part of the chapter there is a description of these and a graphic example for each of them. There is also a brief hint on how to try to eliminate them directly during the sampling of the signal. Next there is a description of the independent analysis of the components, a technique that will be used for the removal of artifacts. In my thesis, I focused particularly on the removal of the eye blink. An artifact that manifests itself during the closing of the eye. In the description of this technique there is a particular attention to the parameters required by the algorithm and an overview of its advantages and limitations.
- In the fourth chapter there is a description of cross-frequency coupling, CFC, a technique through which to study the interaction between the different bands of the EEG signal. In fact, several studies have noted how there is a relationship between the different frequency rhythms. CFC can be studied through

different couplings, but the most used one is PAC, i.e. phase-width coupling, which is believed to be responsible for the integration of neuron populations. In this chapter there is an overview of the steps to be taken to obtain the CAP, including the extraction of bands and phase and amplitude. Finally, the main methods of coupling analysis documented in the literature are presented critically.

- The fifth chapter summarises the results of the work. At the beginning there is the description of the dataset used, which, as already mentioned, is about 15 epileptic patients. In particular they are EMA subjects, i.e. with eyelid myoclonia with absences. In the second section of the chapter there are the results related to the removal of the artifacts. The analysis of the independent components was then applied to the recorded signals, obtaining clean signals that could be used for the next work. The signals I worked on are EEG signals recorded inside the fMRI, so they are not easy to clean because they are corrupted by multiple external noises. In the last part of the chapter there are the results of the application of the PAC to the cleaned signals. In particular, in this case I studied the coupling between alpha and gamma band frequencies, as several studies have shown their close interaction in different pathologies.
- Finally, in the last chapter there is a quick look at possible future work. That is, after studying how the different frequency bands interact between the various channels within the EEG, one can go and study functional connectivity. This technique instead studies the interaction between different parts of the cerebral cortex.

Chapter 2

Electroencephalographic signal and Epilepsy

Electroencephalography, EEG, is an electrophysiological screw-up procedure to record the electrical activity of the brain. This technique is non-invasive, and electrodes are placed along the scalp.

At the end of the nineteenth century the English physiologist Richard Canton and the polish Adolf Abraham Beck were the first to discover the electrical activity of the brain. Canton was the first to record a negative variation in brain potential on rabbits and monkeys, in this case he used an optical stimulus through a flame. The physiologist finally observed that this signal was recorded in the hemisphere opposite the illuminated eye. [1]

The first real recording of human brain activity occurred in 1927 by a German neurologist Hans Berger who placed the electrode son an intact and flawless human scalp. The term electroencephalogram in reference to the electrical signal of the brain appears for the first time on an article in 1929 also by Berger himself.

Early EEG studies showed that the recorded activity changed depending on the functional state of the brain such as sleep, oxygen deficiency or certain pathological conditions such as epilepsy.[2] In recent years EEG traces have assumed a primary and clinical role in areas such as neurology, neurosurgery and psychiatry. The potentials recorded are an expression of the electrical activity of excitable brain cells called neurons. An example of excitable cells are some nerve and muscle cells. They are defined excitable because they are able to generate rapid electrochemical pulses at membrane level, used to transmit signals at membrane level. In fact, starting from the resting potential, under certain conditions, they can be excited producing an action potential.

2.1 Nervous System

The nervous system, so called because it is composed of organs formed by nervous tissue, is responsible for the reception of external and internal stimuli and the elaboration of coordinated effective reactions of voluntary and involuntary type. Complex psychic functions such as memory, learning and emotions are also associated with it.

The nervous system can be divided into central nervous system, CNS, consisting of the brain, enclosed in the cranial box, and by the spinal cord, contained in the vertebral canal, while the peripheral nervous system, PNS, formed by the nerves.

The CNS has many purposes, in fact, it is responsible for human perceptions and feelings, voluntary decision-making and thinking. Furthermore, its main function is to maintain homeostasis, that is the tendency to resist change in order to keep a stable internal environment; by doing so, the CNS coordinates the activity of all human organs. It is very vulnerable to physical trauma and it is protected and supported by glial cells, cerebrospinal fluid, CSF, connective tissue, and bones. [1]

The PNS provides the connection between the CNS and the organs and the limbs. Not being protected by any barrier, it is much more exposed to possible injuries. The PNS is divided into the somatic, the sensory and the automatic nervous system. The autonomic nervous system is the part of the PNS responsible for controlling the functions of internal organs and some muscles. The somatic nervous system, on the contrary, has primarily a function of transporting information related to voluntary movement and sensory information.

2.2 Central Nervous System

As previously mentioned, the central nervous system plays many key roles within our system but is very vulnerable to physical trauma. In addition, the most external structures that provide physical support to the CNS are the cranium, which connects the brain, and the vertebral column, which surrounds the spinal cord. However, these two structures can represent a mechanical risk for the CNS, in fact, in case of impact, their rigidity could damage the extremely delicate nervous tissue. Because of this problem, the CNS receives additional protection from the *meninges* and *cerebrospinal fluid*.

The meninges are three layers of connective tissue surrounding the brain and spinal cord. The outermost membrane is the *dura mater*, made of tough fibrous tissue, the middle layer is the *arachnoid mater*, because of its shape, and the innermost membrane is the *pia mater*, characterized by softer tissue. Between the arachnoid and the pia mater is the subarachnoid space, a cavity that is filled with cerebrospinal fluid. This body fluid is also found in other cavities of the brain and surrounds the neurons and glial cells.

2.2.1 Cells of CNS

The Central Nervous System, CNS, is composed by two principal classes of cells: neurons and glial cells. All these structure will be described in details in the following paragraphs.

Neurons

The neurons represent the anatomic-functional unit which can perform excitability and electrical-pulse transmitted communication in a network.

They have ion channels embedded in the membrane which are selective to specific ions such as Na^+ , K^+ , Cl^- and Ca^{++} . If the voltage changes by a large enough amount, an "all-or-none" electrochemical pulse, called action potential, develops.

The neuron, thanks to its chemical and physiological properties, is the cell responsible for the generation, processing and transmission of nerve impulses. Neurons form a dense communication network through which information is exchanged from the nervous system to other organs and conversely.

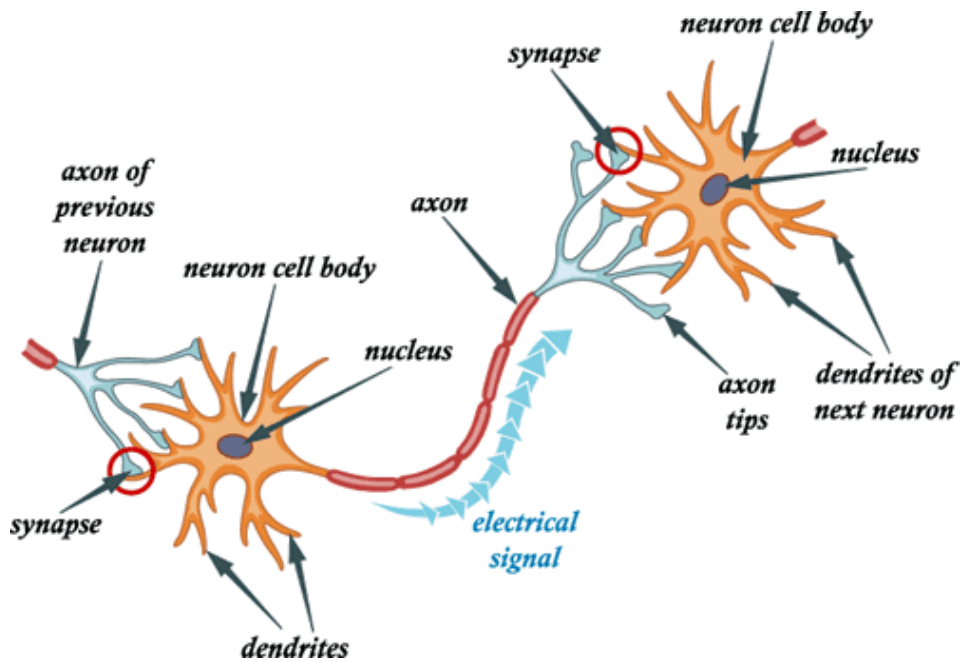


Figure 2.1. *Structure of neurons*

From the anatomical viewpoint, neurons consist of three components (see Figure 2.1):

- a compact cell body, or *soma*, containing the nucleus and intracellular organs
- *dendrites* that branch off the nucleus and receive information from other neurons thanks at the synaptic junctions
- a single *axon* another neural fiber extruding from the soma that is in charge of sending information to multiple neurons. The axon terminal contains synapses, specialized structures where neurotransmitter chemicals are released to communicate with target postsynaptic neurons. [2]

From the functional point of view it is possible to classify neurons in three categories: afferent or sensory neuron, efferent or motor neuron and interneurons. The first ones are the neurons that transmit signals from the sensory organs to the CNS. The efferent neurons transmit motor signals to the peripheral organs. Finally, the interneurons are present exclusively in the CNS and integrate the information between afferent and efferent neurons.

Glial cells

Glial cells, or neuroglia, represents the 70-90% of the total number of cells of the CNS. This cells have a lot of mansion but their principle role is to provide mechanical support to neurons (see Figure 2.2).

There are different types of neuroglia, among which the most important are astrocytes and microglia.

Microglia are phagocytes responsible of protecting the CNS from bacteria and cellular debris; they also protect neurons from oxidative stress. They comprise approximately the 15% of the total cells of the CNS.

Astrocytes are a particular star-shaped cells that are very differentiated and thus are able to perform several tasks in the CNS. They play an important role in the maintaince of the extracellular environment balance by removing excess ions, in particular potassium. Moreover, they provide physical and nutritional support for neurons, and regulate the development and regeneration of synapses and axons and provide biochemical support of endothelial cells forming the blood-brain barrier.

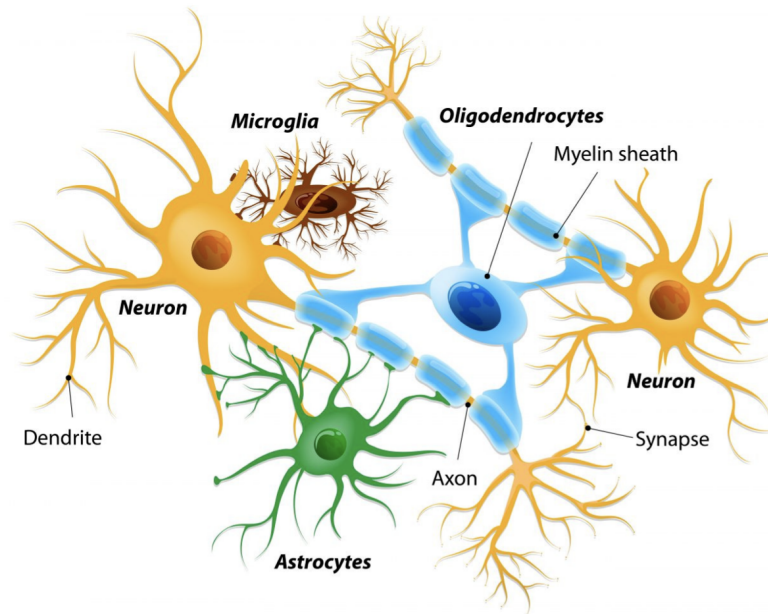


Figure 2.2. *CNS cells: interaction between neurons and neuroglia*

Neural arrangement is really clearly definite in the CNS. Cellular bodies, dendrites and axon terminals form clusters that appear grey to the eye, and axons form white agglomerates. grey substance takes about 40% of CNS and is the place where integration of knowledge occurs. white matter occupies the remaining 60% and is responsible for quick transmission of data. The brain is covered by a layer of gray matter, called cerebral cortex; white matter is found below and features small clusters of grey substance underneath, called subcortical nuclei.

2.2.2 Synapse

The passage of information between successive neurons occurs at the synaptic space level. A synapse can be considered as a particular cell junction. Through synaptic transmission the nerve impulse propagates from one neuron to another or from one neuron to another type of excitable tissue.

Different structures of the neuron can be coupled in the synapses and, depending on the structures involved, it is possible to distinguish axon-dendritic synapses, where there is communication between the axon of one neuron and the dendritic axis of another neuron, axon-axon synapses, where there is communication between two axons and axon-somatic synapses, where there is communication between the axon and the soma of the two neurons.

Two different categories of synapses are distinguished:

- *Chemical synapses* composed of three elements: presynaptic terminal, synaptic space and postsynaptic terminal (see on the left of Figure 2.3). They are characterized by the presence of neurotransmitters. In order to be functional, the neurotransmitters, released from the presynaptic terminal, must cross the synaptic space and connect to the receptors of the postsynaptic terminal and this determines the so-called synaptic delay. Another characteristic of this type of synapse is the unidirectionality of the information passage. In this synapse the neurotransmitter is inserted into structures called synaptic vesicles. When the membrane of the presynaptic neuron depolarizes, the voltage-dependent calcium channels present in it will open, causing calcium ions to flow inside the terminal, this ion flow triggers the process of opening the vesicles and the neurotransmitter is released into the synaptic fissure.
- *Electrical synapses* in which the cytoplasm of the presynaptic cell and that of the postsynaptic cell are in close contact, thanks to the presence of specialized ionic channels, called gap junction (see on the right of Figure 2.3). The gap junctions allow the direct passage of electrical currents, eliminating the synaptic delay present in chemical synapses. Moreover, they generally allow conduction in both directions.

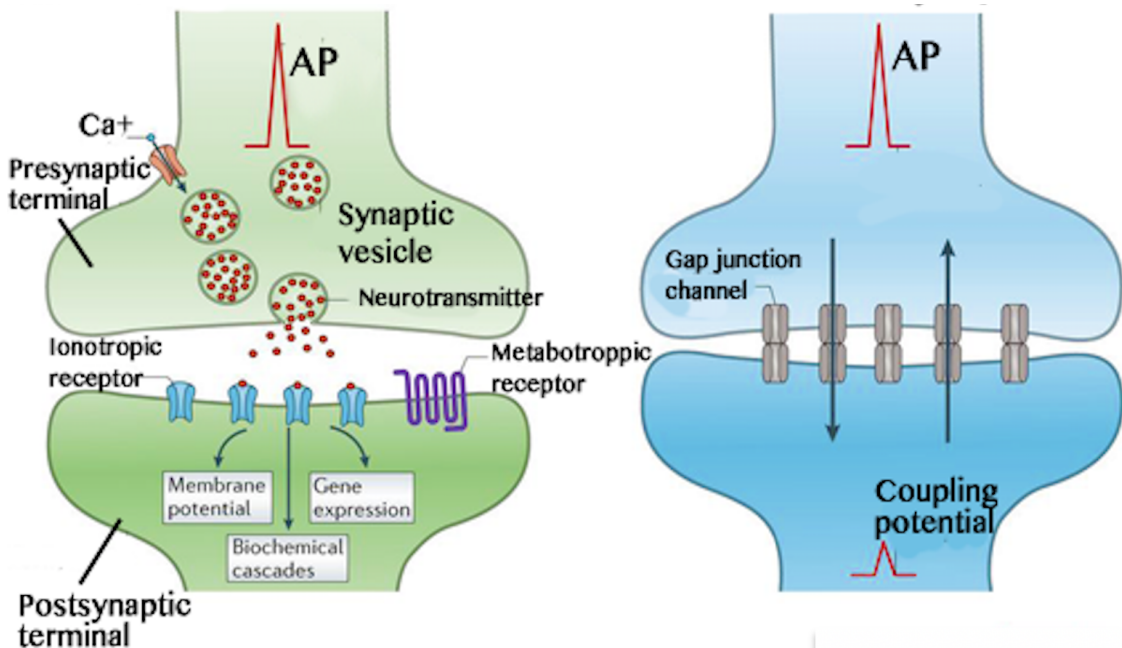


Figure 2.3. *Functional anatomy of a chemical synapse (on the left) and an electrical synapse (on the right)*

2.3 The human brain

The brain is composed of the forebrain, the cerebellum and the brainstem; the forebrain includes the brain and the diencephalon. The brain, or cerebrum, is a C-shaped organ divided into two parts, called hemispheres, by the longitudinal fissure (Figure 2.4). The cerebral hemispheres are made of white matter and surrounded by a thick layer of gray matter, the cerebral cortex. White matter occupies about 60% of the central nervous system and is responsible for the rapid transmission of information. The integration of information occurs in the gray matter, of which the basal ganglia are also made. As for the spinal cord, the arrangement is different: the white matter lies outside and is supported by the gray matter.

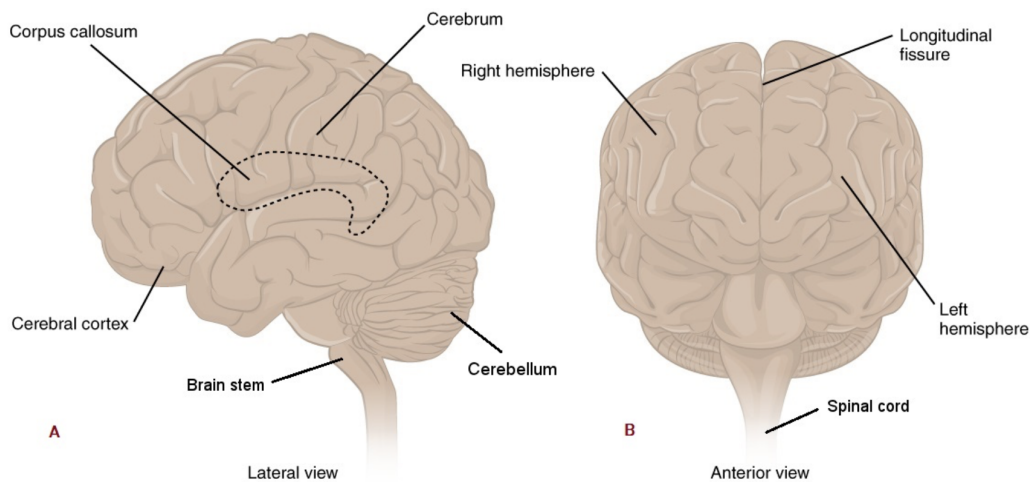


Figure 2.4. *The encephalon. A) Lateral view of the encephalon, brainstem and cerebellum are shown. B) Anterior view of the encephalon: it is possible to observe the two emispheres and the longitudinal fissure*

Diencephalon

Diencephalon is placed just below the brain and consists of two medial structures: the thalamus and iphotalamus. The thalamus is positioned above the hypothalamus and below the cerebellum. It is an aggregation of subcortical nuclei and it plays a significant role in sensory processing and motor control. In fact, sensorial information in order to reach the cerebral cortex passes through the thalamus, where it is filtered and modified. The iphotalamus is found below the thalamus; it is responsible for homeostasis and ensures communication between the nervous and endocrine systems. It is mostly subjected to the control of the autonomic nervous system, for this reason, it releases hormones from the anterior and posterior hypophysis in response to electrical or chemical signals.

Brain stem and cerebellum

The brainstem and cerebellum are found in the posterior area of the skull. The brainstem is a small structure located in the hindbrain; this last one accounts for around 10% the total volume of the brain but contains about 50% of the total number of brain's neurons. It consists of the mesencephalon, the medulla oblongata and the pons. The brainstem plays a fundamental role in the regulation of sleep-wake rhythms and consciousness. The cerebellum, instead, is a bilateral symmetric structure; it is responsible of balance, motor coordination and motor control.

In the next section there will be the treatment of the cerebral cortex with particular attention to functional areas.

2.3.1 Cerebral cortex and functional areas

The most superficial layer of the brain is the cerebral cortex, which is about 2-4 mm thick and consists of the cellular bodies of neurons, glia and myelin-free nerve fibers. The cerebral cortex is the outer layer of grey matter in the cerebrum. It is responsible for the integration of sensory impulses, directing motor activity, and controlling higher intellectual functions.

There are two major furrows: the central sulcus and the lateral sulcus and they divide the cortex into four areas: the occipital, temporal, parietal and frontal lobes (see the Figure 2.5).

In the following there is a description of this areas.

Frontal

Located in the front of the head, just below the frontal bones of the skull and near the forehead, it forms the dominant part of our brain. The frontal lobe is the section responsible for personality, language and motor control. It consists of the primary motor cortex, which is involved in the generation of volitional movements and the execution of tasks requiring attention, the prefrontal cortex, the pre-motor cortex and the additional motor area. Among the different functions it can perform, we find the production of language and speech, thanks to Broca's area and the area that deals with understanding and reacting to the feelings of others, empathy then.

Temporal

The temporal lobe is found in both emispheres, it is located beneath frontal and parietal lobes, and it is separated from the former by the lateral sulcus. It is also responsible for a large number of cognitive processes. They participate in many sensory and intellectual functions, such as auditory perception, olfactory perception, learning and declarative memory, so they can be considered the actual seat of intelligence. Going to analyze specifically, in the superficial lateral part, there is

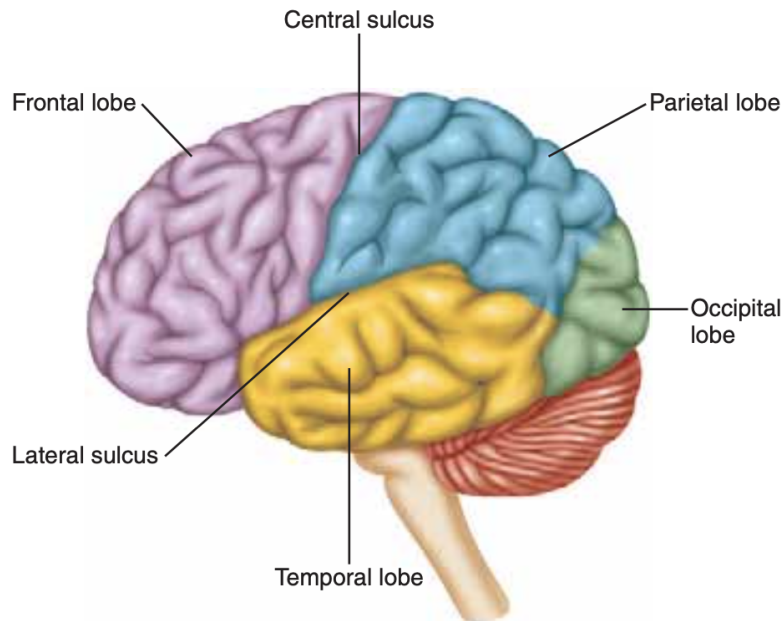


Figure 2.5. *Lobes of the cerebrum.* This lateral view of the left cerebrum shows its four distinct lobes: frontal, parietal, occipital, and temporal

the auditory cortical area and the nerve centers responsible for the understanding of spoken language. In the deep part there are other areas and structures involved in mnemonic and emotional processes. The anterior and basal areas of the lobes, together with the rest of the limbic system, are responsible for the transmission and processing of olfactory stimuli, and are involved in emotional and affective processes. One of the main functions of the temporal lobes is the recognition of sound and visual stimuli, such as spoken language, music and images.

Parietal

The parietal lobe is located above the temporal lobe and behind the frontal lobe. This area is called somatosensory cortex. Its functions are multiple, but what defines this cerebral area is mainly its role in sensory and spatial perception, body movement and sense of orientation. In this lobe, information about most of our sensory organs is also captured. Here, pain as well as physical exertion and body temperature are processed and modulated. On the left side, the predominant hemisphere, the lower parietal area is responsible for mathematical functions and is closely related to language recognition and word memory. In the non-dominant hemisphere, the right part, is in charge of visuospatial activities, i.e. non-verbal activities.

Occipital

The occipital lobe is located in the back of the brain and its main activity is to process vision, in fact it is also referred to as the visual cortex. Inside it there are many neurons specialized in the recognition and processing of the details of an image. Among the 4 brain lobes, the occipital one is the smallest, but also the most interesting. It is located near the nape of the neck and has no real function. Rather, it is almost like the way of connection and organization of most mental processes. In detail it has a key function for the sense of sight, helps to distinguish colors and participates in the processing of emotions and thoughts.

Through imaging it has been seen that each lobe in turn is divided into several regions, each of which has a specific function such as the primary motor cortex, the associative sensory cortex and the associative visual cortex. Many different areas are connected to each other so that they can also perform associative functions. Summarizing, many cortical areas are dedicated to the processing of sensory information or the generation of motor commands, instead, other areas play a central role in complex cognitive mental mechanisms or functions such as thought, awareness, memory, attention and language.

2.4 EEG

Electroencephalography, as previously mentioned, is an electrophysiological technique used to monitor the electrical activity of the brain. Although EEG is a technique that lacks a good spatial resolution, at the same time it offers an exceptional temporal resolution, around ms, and therefore is widely used in diagnosis. For example, it is used to investigate epilepsy, sleep disorders, coma and brain death. The standard EEG method is based on a non-invasive approach; several electrodes are applied directly to the scalp and record for a certain period of time the spontaneous electrical activity from the brain.

EEG is used to record the synchronized activity of large populations of neurons; the different waveforms that are obtained, specifically, are given by the overlapping field potentials produced by each single neuron belonging to a certain brain volume. The EEG can be used to have an evaluation of the functional state of the brain in particular conditions of activation to which the subject under examination is subjected, both during wakefulness and during sleep.

2.4.1 Feature

The electrical activity of the EEG signal, in the practical treatment, is studied as a random signal because it is generated by a very high number of neurons that are rarely operating synchronously in the same instant.

There are some parameters to consider in the analysis phase and they are:

- Amplitude: variable between a few μV to a few hundred μV . It can be divided into 3 bands: low $<30\mu\text{V}$, medium 30 - 70 μV and high $> 70 \mu\text{V}$
- Frequency: included in a band ranging from a few Hz, about 0.5 Hz up to 80 Hz. Despite this, much of the useful information of the EEG signal is contained in a narrower band, 40 Hz
- Symmetry: relative to the presence of the signal in both hemispheres. If the signal is present in only one hemisphere, then asymmetry will be discussed
- Synchronicity: relative to the moment of appearance of a certain electroencephalographic event. If the events occur simultaneously in the two hemispheres, they are synchronous, otherwise asynchronous
- Topography: defined as a function of the brain areas in which the potential is manifested
- Morphology: can be polymorphous or monomorphous. A polymorphic signal is a signal characterized by the succession of potentials belonging to the same frequency band, but with irregular frequency and amplitude often different from one component to another. A monomorphic signal, instead, is a signal characterised by the regular succession of potentials at the same frequency and amplitude

2.4.2 Frequency bands

EEG recordings show that brain electrical activity has a continuous and oscillatory character. The waveforms and their amplitudes are functions of the overall excitation of the brain, in fact the amplitude of brain waves depends on the degree of synchronization with which the cortical neurons interact with each other.

As shown in the Table 2.1, in the EEG the values assumed by the wave frequencies fluctuate between 0.5 and 100 Hz, progressively increasing as cortical activity increases, but in general most of the information content is within 40 Hz.

The harmonic composition of EEG signals is generally complex, in particular, five types of rhythms can be distinguished: alpha waves (α), beta waves (β), theta waves (θ), delta waves (δ) and gamma waves (γ).

Band	Hz
Delta	0-4
Theta	4-7
Alpha	8-13
Beta	13-30
Gamma	30-100

Table 2.1. EEG signal rhythms

Next we will describe the rhythms and show the characteristics of each of them. A typical example of a pattern will be shown for everyone. [2]

Delta

Delta waves have a frequency between 0.5 - 4 Hz and an average amplitude of $75 \mu\text{V}$. In adults, δ waves are associated with deep sleep states, while great δ band activity in the waking state is considered a pathological state. In children, the δ wave amplitude decreases with increasing age.

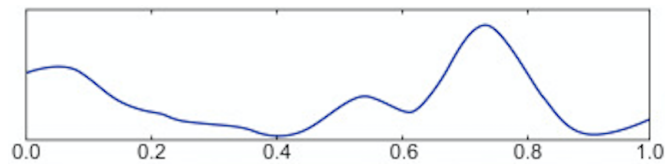


Figure 2.6. Example of Delta wave

Theta

Theta waves have a frequency between 4 - 7 Hz and an average amplitude of $150 \mu\text{V}$. These theta waves are also more present in children, while in adults they are associated with states of sleep or meditation. In particular, in adult subjects appears in the presence of many brain diseases and in states of emotional tension and hypnosis.

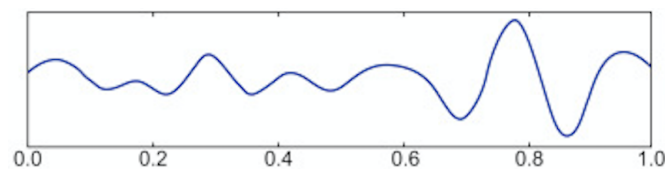


Figure 2.7. Example of Theta wave

Alpha

Alpha rhythms have oscillations at frequencies between 8 - 13 Hz and voltage amplitude between 20 - 200 μV .

The α wave is the most commonly analyzed signal and is well visible in patients with quiet and resting brain. It was analyzed that if you are in the presence of visual or sensory stimuli the rhythm is greatly attenuated in amplitude and are no longer present in sleep, except for the REM stage.

The alpha rhythm usually presents a regular and continuous pattern, but in

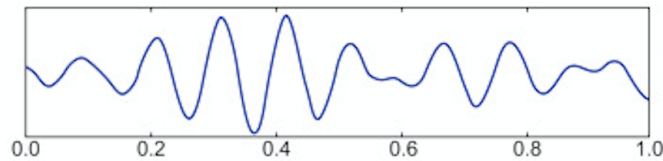


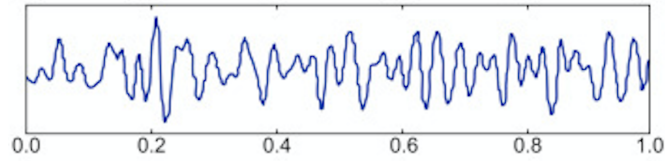
Figure 2.8. *Example of Alpha wave*

some individuals it can be very irregular and not always present, in fact it often disappears or occurs only occasionally. It is generated with greater intensity in the occipital area, which is the same area where the signals coming from the retina are received and processed, and it is for this reason that the alpha signal is greatly attenuated in the presence of a visual stimulus.

This characteristic is easily observable by making the subject close-and-open his eyes; in fact, when an individual, psychically and physically at rest, opens his eyes, the voltage of the alpha rhythm is lowered, even to disappear completely. Normally, if the eyes remain open, it does not return regularly but appears occasionally for some time, and if the subject also undertakes a mental activity, the rhythm is greatly reduced until it disappears completely. [3]

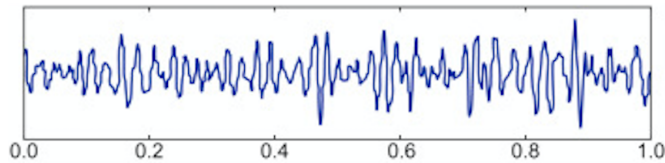
Beta

The beta rhythm has a frequency between 13 - 30 Hz and an amplitude of about 5-10 μV . They are generated with greater intensity in the parietal and frontal lobe regions. Within the frequency range of the beta rhythm it is possible to distinguish between two sub-bands: the slow- β with frequencies between 13 and 18 Hz and the fast- β with frequencies between 18 and 30 Hz. Specifically, the slow- β is influenced by mental activity, while the fast- β is characteristic of situations of stress and intense CNS activity. In general, β rhythm is associated with levels of consciousness such as attention and concentration.

Figure 2.9. *Example of Beta wave*

Gamma

This rhythm has a frequency between 30 - 100 Hz, with low voltage amplitudes and is related to the highest cognitive processes. In many studies it has been seen that gamma rhythm plays a fundamental role in memory formation.

Figure 2.10. *Example of Gamma wave*

2.5 The International 10-20 System of Electrode Placement

When recording the EEG signal, an electrode application standard is used. In particular, the most used is the International 10-20 System of Electrode Placement which is an internationally applied model. It was established to have standardized measurements and methods in the scientific community and to ensure the reproducibility of the results of clinical and research studies.

This system is a symmetrical matrix of electrodes placed on the scalp at a distance of 10% or 20% of a reference distance (Figure 2.11). The reference distance is often taken as the distance between two cranial points: inion and nasion, where the nasion is the depressed area below the forehead between the eyes, the inion is the occipital protuberance located in the lower area of the human skull.

Each group of electrodes carries a label that indicates the area of the brain from which the biopotential is recorded, the principal are: FP - prefrontal, F - frontal, T - temporal, C - central, P - parietal, O - occipital. A number must be added to the letter, so that odd numbers refer to the left half of the skull and even numbers to the right half while Z sites correspond to electrodes positioned along the midline of the sagittal plane of the brain.

The measuring electrodes are applied to the scalp with the aid of double-sided adhesive tape, plasters or by using a special cap on which the electrodes can be alloyed. They must be applied in a stable manner so that they are as immune as possible to external interference.

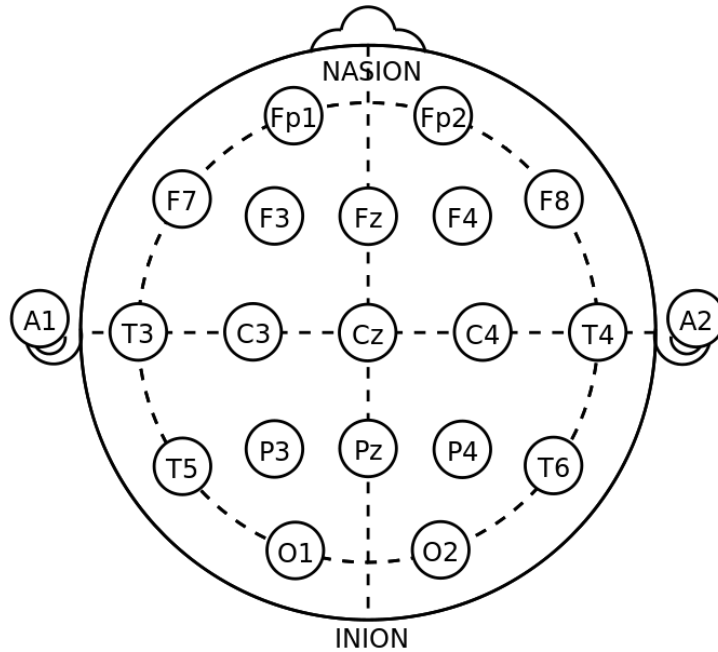


Figure 2.11. *Electrode placement system according to the international standard*

The conventional EEG, so the one that uses 21 electrodes, as can be seen in the figure 2.11, suffers from spatial resolution problems because it uses electrodes that have a spatial resolution of about 1-2 cm, so it also detects the activity of the area adjacent to the one below. Since the recorded signal is given by the sum of the detected electric fields, this does not allow to trace the exact origin of the cortical potential. There is the possibility to use a system with 256 electrodes, and in this way it is possible to have a better spatial localization, while maintaining good temporal resolution. These new EEG sampling techniques are defined at high spatial resolution and allow to obtain a high spatial sampling.

To obtain the electroencephalographic signal, the signals from the electrodes are sent to a differential amplifier, and the connection between electrode pairs and the inputs of these amplifiers is the assembly.

From the figure 2.12, it can be observed that there are two types of recording [4]:

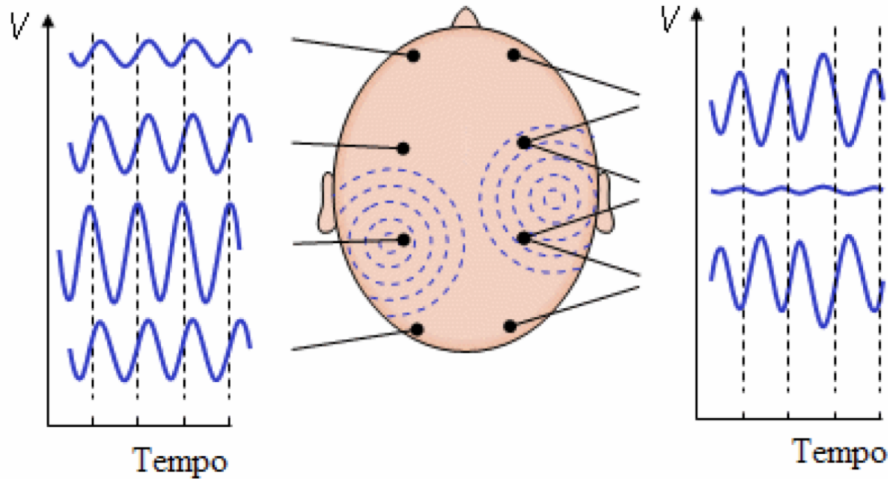


Figure 2.12. *Example of monopolar (left) and bipolar (right) derivation*

- monopolar recording: one electrode is placed in an active site, while the other, called the reference electrode, is placed in an electrically neutral site, which can be for example the tip of the nose, the ear lobe, the chin. With a unipolar reading, the potential of each electrode is measured against the neutral electrode or the average of all electrodes. This type of recording therefore highlights the absolute level of electrical activity below the active site.
- bipolar recording: in this case both electrodes are placed on active sites in the area of interest and the signal detected corresponds to the difference that emerges between the activities of the two sites. [5]

2.6 Functional Magnetic Resonance - fMRI

In 1992 the technique of functional magnetic resonance imaging was applied for the first time to humans. It is a method used to investigate the operation of the central nervous system, in a complementary way to morphological investigations.

The instrument of fMRI is of crucial importance in the neurological field and makes it possible to locate brain activity with good temporal accuracy, but above all with millimetric spatial resolution. [6]

The fMRI measures the variation of blood oxygenation over time through the reconstruction of the BOLD signal, an acronym for Blood Oxygenation Level Dependent, i.e. it is a measurement of the level of blood oxygenation, which varies

according to the metabolic demand of active neurons. The marker used to study the activation of brain areas is hemoglobin. In fact, it behaves differently if it is in an oxygen-related or oxygen-free configuration:

- oxygenated hemoglobin, Hb has diamagnetic characteristics, i.e. it has no odd electrons and has zero magnetic momentum
- while deoxygenated hemoglobin dHb is paramagnetic and therefore has odd electrons and magnetic momentum different from zero.

Completely deoxygenated blood is characterised by a magnetic susceptibility, i.e. the intensity of the magnetization of the material, which is 20% greater than that of completely oxygenated blood. The fMRI exploits this magnetic property of hemoglobin, which is therefore used as an endogenous contrast medium.

A first hypothesis is that an increase in neural activity leads to a higher consumption of oxygen and a consequent increase in dHb, which, in turn, would lead to a decrease in the BOLD signal, however, experimental observations show that these relationships are much more complex. In fact, during an increase in nerve activity, not only is there no decrease in the acquired signal, but there is also an increase in the MR signal, Magnetic Resonance, and this indicates that activation causes an increase in blood oxygenation.

There are two main experimental approaches used for the acquisition of the BOLD signal: Block Design and Event Related. [7]

In the Block Design, periods in which stimuli are absent, called rest time, are alternated with periods in which the patient is exposed to stimuli. The latter can be of different nature: cognitive, motor or sensory and are administered repeatedly for a predetermined period of time, followed by a period of absence of stimulus. The advantages of this experimental design are simplicity of execution and SNR improvement.

In the Event Related design several individual stimuli are administered, each of them separated by a stimulus interval that can change from 2 to 20 seconds, or vary from stimulus to stimulus. Representing the response to each individual task, the acquired BOLD signal is considerably weaker than that of a block of stimuli. This experimental design effectively estimates the temporal trend of the hemodynamic response, thanks to the stimulus intervals in which the signal returns to basal condition. Event Related is advantageous in that stimuli can be randomised to prevent subsequent events from being predictable by the patient.

2.6.1 EEG-fMRI

Until now, the EEG and fMRI have been used separately and shown to be of considerable importance for non-invasive studies in both clinical and cognitive neuroscience. The high degree of complementarity between the two techniques has led to the idea of using a multimodal approach in order to exploit one technique to compensate for the deficiencies of the other and vice versa, so as to achieve a greater understanding of the dynamics and structure of brain activity.[8]

As shown in the Figure 2.13 [9] it is possible to notice the importance of the inte-

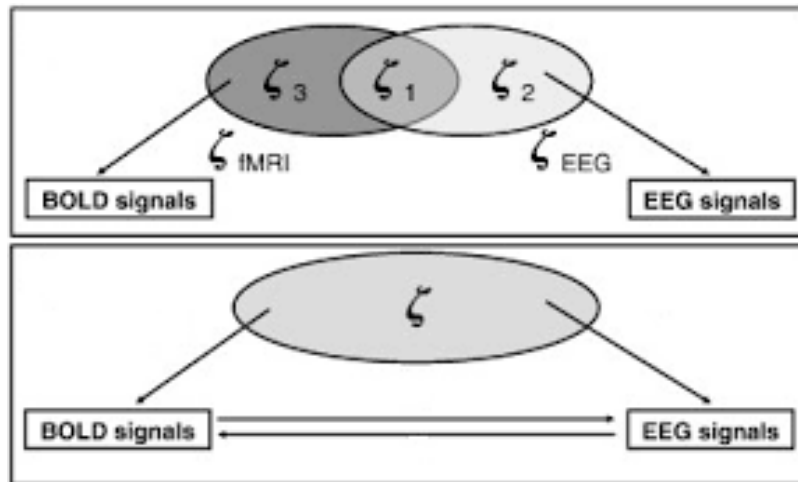


Figure 2.13. *Integration of EEG and fMRI technique*

gration of the two above mentioned techniques. In the image above it can be seen how, using only one technique, part of the brain information is lost. In the picture below there is an extended understanding of brain function and structure.

Recording EEG potential during fMRI imaging identifies brain activity and information on the relative locations of signal generators. The combination of the two signals therefore allows the high spatial resolution of the fMRI to be combined with the high temporal resolution of the EEG.

Generally the coupling of the two techniques is used for the localization of EEG signal sources and the identification of spontaneous EEG activity, used in studies of resting and sleeping activity.

The EEG-fMRI combination is not free from artifacts, in fact they are caused by the interaction of the two instruments, compromising both the quality of the EEG signals and the quality of the resonance images.

2.7 Epilepsy

Epilepsy is the most common chronic neurological disease after migraine; an estimated 50 million people worldwide suffer from it. The incidence varies from 40 to 70 per 100,000 inhabitants per year in industrialised countries and from 100 to 190 per 100,000 inhabitants per year in developing countries.

Epilepsy is a clinical condition characterised by the sudden onset of neurological symptoms due to a sudden, hypersynchronous and simultaneous discharge of a more or less large population of neurons. These discharges always originate from neurons in the cerebral cortex. The neurological symptoms resulting from an epileptic seizure are extremely diversified according to the cerebral area involved and may consist of alterations in the state of consciousness, behavioural alterations and alterations in motor and sensory functions.

The mortality rate in patients with epilepsy is 2-3 times higher than in the general population. Death can be related to epilepsy, i.e. due to tumors, ischemic heart disease, suicide or accidentally occurring during a seizure, asphyxia, accidental injury or drowning.

People affected by epilepsy can be divided into four different prognostic groups [10]:

- Excellent prognosis: includes 20 - 30 % of people who develop epileptic seizures. Usually in these cases there is spontaneous remission.
- Good prognosis: includes 30 - 40 % of people with epilepsy. Remission obtained after pharmacological treatment, which normally remains after therapy.
- Drug dependent prognosis: includes 10 - 20 % of people with epilepsy. This group shows the possibility of remission through pharmacological treatment, the need to maintain the therapy and frequent relapse after its suspension.
- Bad prognosis: includes 20 - 30 % of epileptics. Subjects in this group show drug resistance. They do not cease more careful observation and in some cases surgical treatment is required.

2.7.1 Classification

The classification of the various types of epilepsy has many purposes, in fact, can provide a structure to understand the type of seizures that are present, what other types of seizures could occur in the same subject, the possible triggering factors of the seizures and often their prognosis. In the classification process, the clinician begins by classifying the type of seizure. Later on, the type of epilepsy and, in many cases, the specific epileptic syndrome can be classified.

The following classification of epilepsy refers to the classification of the International League Against Epilepsy, ILAE. [11]

Kind of seizure

The starting point of the classification structure is the type of seizure. On the basis of the initial characteristics, they are classified into focal, generalised and unknown onset. In some situations, in the absence of EEG, video and image studies, the classification based on the type of seizures is the highest possible level for diagnosis. In other cases, the information may not be sufficient for a higher level diagnosis, such as when a patient has had a single crisis.

Kind of epilepsy

The second level of diagnosis is the type of epilepsy. There are mainly four categories: Generalized and Focal Epilepsy, Combined Generalized and Focal Epilepsy and Unknown Type Epilepsy.

In the case of a diagnosis of *Generalized Epilepsy*, the patient's EEG typically shows generalized spike-wave abnormalities. People with generalised epilepsy may have various types of seizures, including absences, myoclonic seizures, atonic seizures, and tonic-clonic seizures. The diagnosis of generalised epilepsy is based on clinical features, supported by the presence of typical EEG intercritical discharges.

Focal Epilepsies include focal or multifocal crises, as well as crises affecting a hemisphere. Various types of focal seizures can be recognised, including focal seizures with or without contact impairment, motor and non-motor focal seizures, and focal seizures that evolve into bilateral tonic-clonic seizures. The intercritical EEG typically shows focal epileptiform abnormalities, but the diagnosis must be based on clinical criteria and supported by the results of the EEG.

Classification into *Generalised and Focal Combined Epilepsy* means that some patients have both generalised and focal seizures. Again, the diagnosis is based on clinical features, supported by EEG findings. EEG documentation of seizures is useful but not essential. Intercritical EEG can show both focal and generalised epileptiform abnormalities, however, epileptiform activity is not essential to make the diagnosis.

The term *Unknown Type Epilepsy* is used to describe patients who have epilepsy but the clinician is unable to define whether the type of epilepsy is focal or generalised due to lack of sufficient information. This may be due to different reasons: EEG not available or EEG not informative.

Epileptic syndromes

The third stage is the detection of Epileptic Syndrome. An epileptic syndrome is defined by the association of specific characteristics including types of seizures and EEG and neuroimaging evidence. Syndromes often have age-dependent characteristics: age of onset, seizure triggers, circadian variations and prognosis. The

definition of a syndrome may also have etiological, prognostic and treatment implications. It is important to note that there is not necessarily a unambiguous correlation between an epileptic syndrome and a diagnosis, and that the definition of an epileptic syndrome may be useful to improve patient management at different levels. There are many well recognised syndromes, such as Epilepsy with Absences of Childhood, West syndrome and Dravet syndrome.

2.7.2 Therapy

As regards pharmacological therapy, most cases of epilepsy are treated by the use of anti-epileptic drugs, AEDs. The choice of drug to be used is based on the type of epilepsy the subject presents, normally the therapy is started with only one FAE preferably among the classic ones with gradually increasing dosage. The effectiveness is evaluated over weeks or months depending on the frequency of the attacks and in case of therapeutic failure, AEDs can be replaced or combined with a second drug. In cases of drug-resistant generalised epilepsy, barbiturates and benzodiazepines are used. The therapy, once started and in the absence of seizures, regardless of the type of epilepsy and the age of the subject, should be continued for at least 2 to 5 years. Suspension of the therapy should be slow and gradual and should not be scaled up further in the event of a reappearance of epileptic abnormalities in the EEG. [10]

As for surgical therapy, this is evaluated for patients with drug-resistant partial seizure epilepsy, where the anatomico-electroclinic analysis has shown a stable and unique origin whose removal does not create new neurological or neuropsychological deficits. There are two types of surgical treatment, resective surgery, which consists of resection of the epileptogenic area, and palliative surgery, which targets patients who cannot undergo resective surgery and aims to reduce the frequency and severity of seizures. For this last palliative approach, the most widely used is the stimulation of the vagus nerve.

Chapter 3

Independent Component Analysis to remove EEG's artifacts

3.1 Artifacts

Although the electroencephalograph is designed to record brain activity, one of the main problems is that it also records other activities that have sources outside the brain. These activities, which can be extra-cerebral or physiological, are called artifacts. Artifacts are disturbances, or noises, that contaminate the signal of interest, making it difficult to determine and extract relevant information of brain origin. In the EEG signal, the most common artifacts appear during acquisition due to a combination of several causes, such as incorrect electrode position, uncleaned skin, electrode impedance, etc. There is also continuous detection of physiological artifacts, i.e. bioelectric signals from other parts of the body such as eye blink, eye movement, heart and muscle activity, that are recorded in the EEG. [2]

The improvement in technology can decrease artifacts of extracellular origin, such as line noise, but biological signals must be removed after the recording process. Through the use of appropriate techniques, artifacts present in the signal can be reduced or eliminated, so that a clean signal can be obtained that allows the useful information to be recognized more clearly and more accurately.

3.1.1 Types of artifacts

Figure 3.1 shows the waveforms of some of the most common EEG artifacts, which will be briefly discussed below along with the predefined methods used to eliminate their effects.

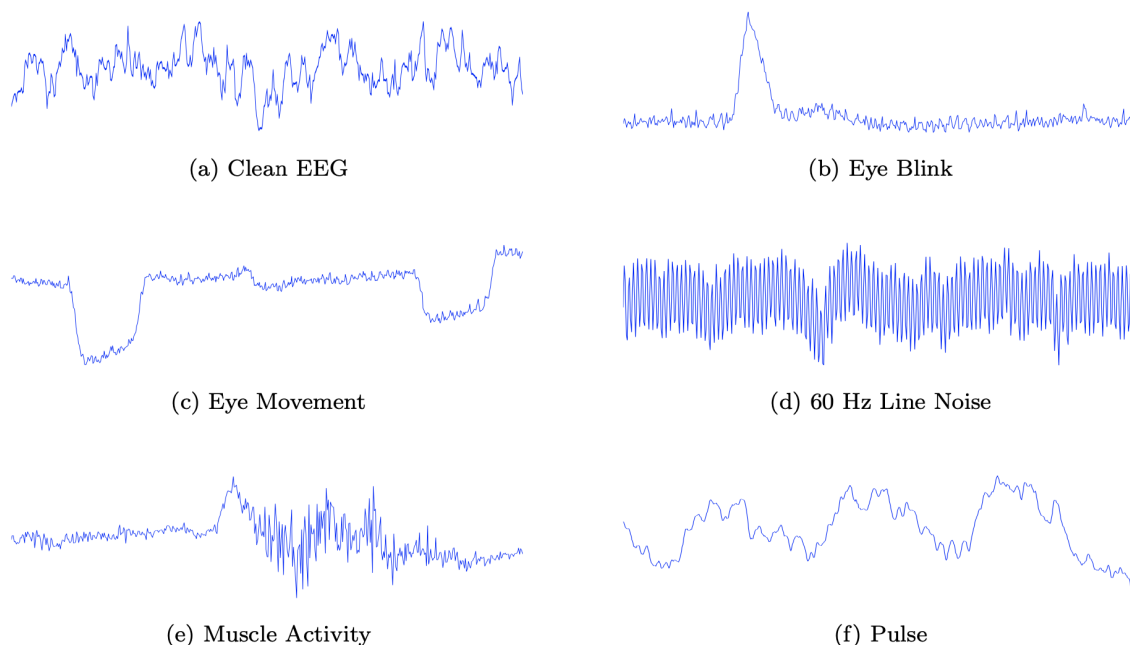


Figure 3.1. *Waveform of some of the most common artifacts in EEG's signal*

Ocular Artifacts

Eye artifacts cause the majority of artifacts in the EEG signal recording. The ocular bulb is a dipole, oriented with the positive pole at the front, corresponding to the cornea. When the eye rotates on its axis, it produces a current field that can be detected by any electrode located near the eye, producing a symmetrically opposite deflection in these electrodes. Therefore, if the electrooculogram (EOG) is available, you may notice that the artifact of the eye is present in the EEG as polarization of the opposite sign to the EOG.

The origin of ocular artifacts is eye movement and eye blink that can spread across the scalp and be recorded by EEG activity. More specifically, eye movement artifacts are produced by changes in the orientation of the retina and dipole of the cornea, and blink artifacts are caused by ocular conduction due to alternating contact of the cornea with the eyelid. [12]

The blink of the eye is characterized by a high amplitude signal that may be greater than the EEG signals of interest (see Figure 3.1.b). This artifact is one of the factors that most degrades the quality of the EEG signal, especially in the frontal channel, but because of its amplitude, a blink can corrupt the data on all electrodes, including those at the back of the head. [13] Eye artifacts are often more directly measured in the electrooculogram (EOG), pairs of electrodes positioned above and around the eyes. Although the exact model of EOG taken through the scalp may be available, it is not possible to simply subtract it from the EEG

signal. Concerning eye movement artifacts (see Figure 3.1.c), its diffusion through the scalp is stronger than that of the eye blink artifact. [14]

The subject is asked to keep their eyes fixed during the recording when possible, however it is not always available for sick subjects or children. The standard method to remove this artifact is to eliminate the signal segment where it appears.

Line Noise

Some sources of artifacts that come from the outside have a negative effect on the EEG measurement. For example, signals from A/C power (see Figure 3.1.d) supplies may corrupt the signal while being transferred from scalp electrodes to the recording device. Line noise may corrupt the data of some or all electrodes depending on the source of the problem. A notch filter centered at the current line frequency is often used to remove this artifact. If line noise or harmonics occur in frequency bands of interest, they interfere with the EEG that occurs in the same band. The notch filter at these frequencies can remove useful information.

Muscle Activity

The contamination of EEG data due to muscle activity is a recognized problem and difficult to manage because it is caused by several types of muscle groups, including neck and face muscles (see Figure 3.1.e).

Typically the myoelectric potentials are characterized by a briefer duration than the brain potentials and are distributed in a higher frequency band, in fact through measurements with electromyogram, EMG it has been demonstrated that it distributes is from 0 Hz to >200 Hz and can be spread over different electrode groups depending on the position of the original muscles. It should be added that EMG contamination and EEG have substantial statistical independence from each other both in time and in space, implying that Independent Component Analysis can be an appropriate metric to remove artifact produced by muscle activity. [15]

Pulse

Cardiac artifacts can be introduced when the electrodes are placed on or near a blood vessel, and are caused by the expansion and contraction movement of the vessel that will introduce voltage variations in the recordings. [16] The artifact signal has a frequency close to 1.2Hz and may appear as a sharp peak or smooth wave, similar to the natural EEG wave, and in case of electrocardiogram, ECG co-recording it can be seen synchronization with it. (see Figure 3.1.f) . One method to remove this artifact may be to use a reference waveform, but there is no standardized method to remove this artifact.

3.2 Blind Sources Separation

The method studied and used for the removal of artifacts is the Independent Component Analysis, ICA. This algorithm is a statistical procedure for transforming an observed multidimensional random vector into components that are statistically as independent from one another as possible. The EEG data consists of recording of electrical potentials in a lot of various location on the scalp and it contains strong undesirable components, deriving from artifacts of physiological or extra-physiological origin.

In order to identify and remove these artifacts is very useful to make an analysis to the independent components. In fact, when this technique is applied to EEG recording, some of the resulting independent components, ICs, represent signals of brain origin while other ICs represent signal of extra-cerebral origin. After the separation of the components, they can be eliminated from the original signals, thus achieving clean signal. This makes ICA a good solution for the identification and removal of artifact from EEG signals [8].

The BSS problem consists in recovering a set of source signals from the observations of their mixtures, without having any information either on the original sources or on how they were mixed. Since no information about the mixing matrix is available, then the linear mixture must be processed "blindly".

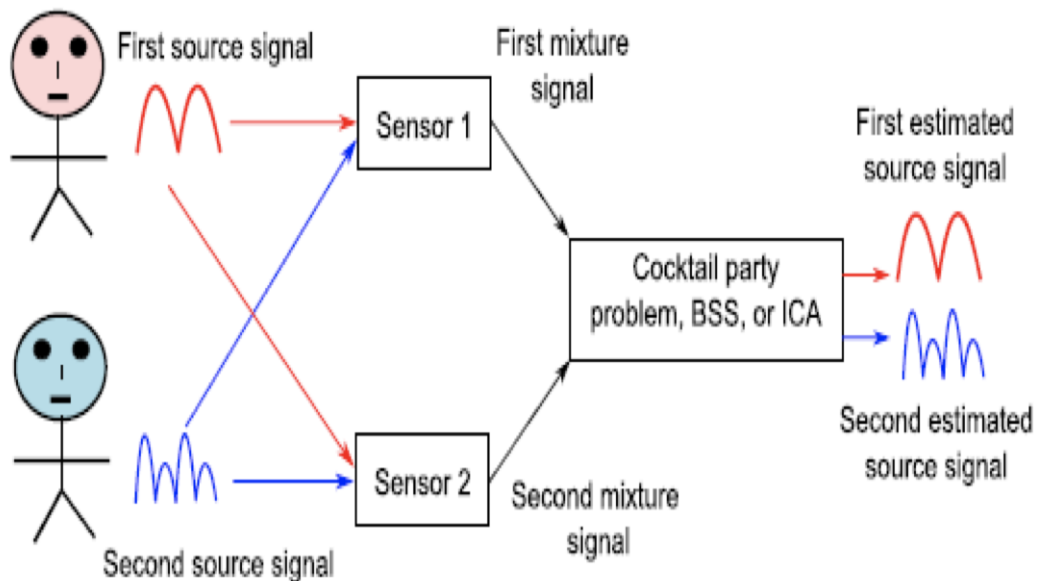


Figure 3.2. *The cocktail party problem*

A classic example of BSS is the Cocktail-Party Problem (see Figure 3.2), in which, for example, is considered a room with two subjects emitting the signals $s_1(t)$ and $s_2(t)$, and two microphones, placed in different positions, which provide two signals $x_1(t)$ and $x_2(t)$, which are recorded in the instant of time t . Each of these recorded signals is a sum of the signals emitted by the two people, then it is possible to express this relationship with a system of linear equations:

$$\begin{cases} x_1(t) = a_{11}s_1(t) + a_{12}s_2(t) \\ x_2(t) = a_{21}s_1(t) + a_{22}s_2(t) \end{cases} \quad (3.1)$$

where a_{11} , a_{12} , a_{21} , a_{22} are parameters dependent on the distance of the microphones from people.

The Cocktail-Party Problem consists in estimating the two original signals $s_1(t)$ and $s_2(t)$ from the recorded signals $x_1(t)$ and $x_2(t)$ only. In case the a_{ij} parameters are known the problem can be solved in a simple way, but in case they are not known the problem is much more complex. The solution to this problem is an algorithm called independent component analysis technique.

There are different models of mixing, subsequently will be treated only linear models that assume the instantaneous mixing of the sources, the signals of interest in a given instant of time are obtained as linear combination of the source signals at that same instant of time.

3.2.1 Definition

Independent component analysis is based on the identification of the sources that maintain most of the information. The analysis of independent component is a technique that allows to estimate $s(t)$ signals from the knowledge of $x(t)$ observations only. Assume to have N different sources simultaneously recorded by M sensors with $M \geq N$, the mathematical model can be described

$$\mathbf{x}(\mathbf{t}) = \mathbf{A}\mathbf{s}(\mathbf{t}), \quad (3.2)$$

where $\mathbf{x}(\mathbf{t}) = (\mathbf{x}_1(\mathbf{t}), \dots, \mathbf{x}_m(\mathbf{t}))^T$ is the $M \times T$ size matrix containing the T samples of the M signals observed, $\mathbf{s}(\mathbf{t}) = (\mathbf{s}_1(\mathbf{t}), \dots, \mathbf{s}_n(\mathbf{t}))^T$ is the $N \times T$ size matrix that contains the T samples of the N source signals and \mathbf{A} are the mixing matrix.

The properties of the mixing matrix \mathbf{A} are briefly shown below [17]:

- Independence: if the signals are shared among the mixtures, then it is independent when the source signals are independent by the mixture signals.
- Gaussianity: gaussianity is a process of mixing signals in a histogram shaped like a bell. This can be used to search for non-Gaussian signals in the mixture of signals. The signals are independently extracted when they are to be non-Gaussian. Therefore signals are estimated independently when they have a fundamental restriction in ICA.

- Complexity: this is more elaborate than the source signals that is shown by the above example of mixed signals. The extracted signals are independent and are non-Gaussian histograms with these signals that represent source signals.

Observing equation 3.2, it can be seen that the linear mixing model has two types of ambiguities [18]:

1. The variance of the individual source signals is not determinable. In fact both \mathbf{A} and $\mathbf{s}(\mathbf{t})$ are unknown and any scalar that multiplies a source signal can be compensated by dividing the corresponding column of \mathbf{A} ; the energy of the single source is placed by convention equal to 1;
2. The order of the sources is not determined. In fact any displacement of the rows of $\mathbf{s}(\mathbf{t})$ can be compensated by the same displacement of the columns of \mathbf{A} .

3.3 Independent Component Analysis

A very common BSS algorithm is the Independent Component Algorithm, ICA. In the ICA algorithm the separation of sources is achieved by imposing their statistical independence.

Assuming the statistical independence and non-gaussianity of the sources, from equation 3.2, it is possible to take advantage of the central limit theorem for the estimate of \mathbf{A} . The goal is to obtain a demixing matrix \mathbf{W} and obtain the independent component simply by:

$$\mathbf{s}(\mathbf{t}) = \mathbf{W}\mathbf{x}(\mathbf{t}) \tag{3.3}$$

where $\mathbf{W} = \mathbf{A}^{-1}$ is the inverse of the mixing matrix. In the ICA model, as mentioned above, only the observations $\mathbf{x}(\mathbf{t})$ are available: the idea is therefore to apply operations to the original data and calculate the independence between the obtained signals in order to reconstruct an approximation of the sources \mathbf{s} .

3.3.1 Assumptions

The independent component analysis model can be used under the following assumptions

- The component \mathbf{s} are statistical independent
- The independent component must have non-Gaussian distribution
- The number of the sources is equal to the number of observations
- The unknown mixing matrix \mathbf{A} is square
- The signals acquired by the sensors are instantaneous linear combinations of the sources

Under the previous constraints the problem is well placed, in fact, the solutions of the problem, the independent components, i.e. are unique, less than the sign, the demixing matrix.

A series of hypotheses are the underlying basis of ICA methods, in fact it is assumed that the signals recorded on the scalp are mixtures of temporal courses of temporally independent cerebral and artificial, that the potentials derived from different parts of the brain, scalp and body are linearly added to the electrodes that the propagation delays are insignificant. When the independent time courses of the various brain sources and artifacts are extracted from the information, the "correct" EEG signals are derived by eliminating the contributions of the artifact sources.

3.3.2 Pre-processing for ICA

There are two main pre-processing strategies in ICA, centering and whitening. These strategies are implemented in order to simplify the algorithm, reduce the dimensionality of the problem and the number of parameters.

- **Centering:** this operation is necessary and simply refers to subtracting the mean vector $\mathbf{m} = \mathbf{E}\{\mathbf{x}\}$, in this way \mathbf{x} became a zero-mean variable. This implies that also the average of \mathbf{s} is zero. The mean can always be re-added to the result the end after estimating the mixing matrix \mathbf{A} with centered data.
- **Whitening:** this strategy reduces the complexity of the problem and the dimension of the data. The idea is to transform the vector \mathbf{x} into a new vector $\hat{\mathbf{x}}$ which is white, so its components are uncorrelated and their variances equal unity. In other words, after whitening, the covariance matrix of $\hat{\mathbf{x}}$ is equal to the identity matrix $\mathbf{E}\{\hat{\mathbf{x}}\hat{\mathbf{x}}^T\} = \mathbf{I}$.

A method for whitening is to use EVD, the eigenvalue decomposition, of the covariance matrix $\mathbf{E}\{\hat{\mathbf{x}}\hat{\mathbf{x}}^T\} = \mathbf{E}\mathbf{D}\mathbf{E}^T$, where \mathbf{D} is the diagonal matrix of the eigenvalues and \mathbf{E} is the orthogonal matrix of eigenvalues of $\mathbf{E}\{\mathbf{x}\mathbf{x}^T\}$. The whitening can be performed by

$$\hat{\mathbf{x}} = \mathbf{E}\mathbf{D}^{-1/2}\mathbf{E}^T\mathbf{x} \quad (3.4)$$

where $\mathbf{D}^{-1/2}\mathbf{E}^T$ is the whitening matrix. Substitute equation (3.2) in equation (3.4), we obtain:

$$\hat{\mathbf{x}} = \mathbf{E}\mathbf{D}^{-1/2}\mathbf{E}^T\mathbf{A}\mathbf{s} = \hat{\mathbf{A}}\mathbf{s} \quad (3.5)$$

Applying this pre-processing you get a new mixing matrix $\hat{\mathbf{A}}$ that is orthogonal.

3.3.3 Measurement of non-gaussinity

As mentioned before, in the BSS model only the $\mathbf{x}(\mathbf{t})$ (Equation 3.3) observations are accessible: the main idea is therefore to apply some adjustments to the original data and measure the dependence between the signals obtained to reconstruct an approximation of the sources $\mathbf{s}(\mathbf{t})$. According to the central limit theorem, the distribution of a sum of independent random variables tends to be toward a Gaussian distribution: in order to separate independent sources, Gaussianity should be minimized.

There are several measures of non-Gaussianity, below are proposed the most common ones [18]:

Kurtosis

Kurtosis is the statistical fourth moment standardized by the square variance. The index of kurtosis of a causal variable with average null v is defined as:

$$K(x) = E \left[\left(\frac{x - \mu}{\sigma} \right)^4 \right] = \frac{\mu_4}{\sigma^4} \quad (3.6)$$

where, μ_4 is the fourth central moment and σ is the standard deviation. Equation (3.6) can be rewritten as:

$$K(v) = E[v^4] - 3(E[v^2])^2 \quad (3.7)$$

For a gaussian distribution the equation (3.7) and the fourth moment $3(E[x^2])^2$ goes to 0, while for non-Gaussian it is different from 0. It is clear that the greater the value, the more the variable considered is different from a Gaussian distribution.

As shown in the figure 3.3 below variables with a kurtosis value greater than 0 are called super-gaussian and present a leptocurtic distribution, variables with a kurtosis value less than 0 are called sub-gaussian and have a platycurtic distribution.

Super-gaussian random variables usually have a spiky probability density function (pdf for short) with heavy tails, i.e. the pdf is relatively large at zero and large variable values, while it is small for intermediate values. Sub-gaussian random variables, on the other hand, generally have a flat pdf, which is quite constant near zero, and very small for larger values of the variable. [18]

The main problem with kurtosis is that can be very sensitive to outliers. Its value may depend only on some observations in the distribution queue, which may be incorrect or irrelevant. In other terms, kurtosis is not a robust measure for the non gaussianity. [19]

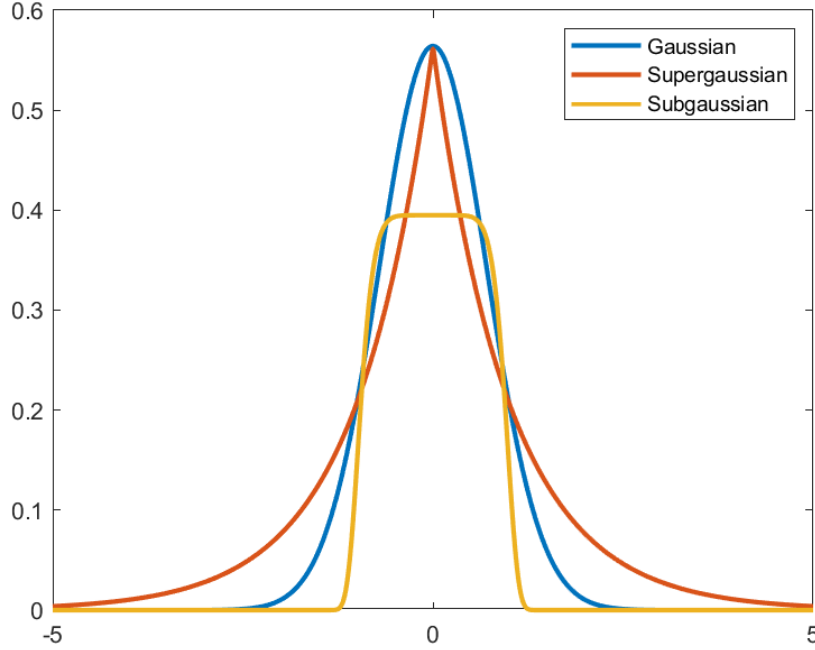


Figure 3.3. *Gaussian, sub-gaussian and super-gaussian distributions*

Negentropy

Considering the covariance matrix of a random variable, negentropy is defined as the difference between the entropy of a Gaussian random variable with the same covariance matrix and the covariance matrix of the considered random variable. Entropy is small for distributions that are sharply focused on certain values, i.e. when the variable is clearly grouped, or has a very spiky pdf. A Gaussian random variable has a value of entropy greater than any random variable of identical variance. [20] This implies that entropy can be interpreted as the amount of information needed to describe a variable; the higher the randomness of a variable, the higher the value of entropy. To obtain a measure of non-Gaussianity that is zero for a Gaussian variable and always not negative, often a slightly modified version of the definition of differential entropy, called negentropy, is used. Entropy, from a mathematical viewpoint, given a random variable v with probability density $p(v)$ is defined as

$$H(v) = - \int p(v) \ln p(v) dv \quad (3.8)$$

Defining a random Gaussian variable that presents the same covariant v_{gauss} matrix, negentropy can be defined as

$$N(v) = H(v_{gauss}) - H(v) \quad (3.9)$$

According to a theoretical point of view negentropy is the best estimator of gaussianity, because it considers all the statistical moments, but it presents a high computational cost due to the fact that it is necessary to calculate the density function of probability of an unknown random variable [18].

Mutual Information

It is possible to define the mutual information I between m random variables, by using concept of differential entropy, such as

$$I([v_1, \dots, v_m]) = \sum_{i=1}^m H(v_i) - H(v) \quad (3.10)$$

The mutual information is a measure of dependence between random variables, it is always not negative and equal to zero if the variables are statistically independent. Suppose having 2 independent variables v_1 and v_2 , the entropy is defined as

$$\begin{aligned} H(v_1, v_2) &= - \int p(v_1, v_2) \ln p(v_1, v_2) dv_1 dv_2 = \\ &= - \int p(v_1)p(v_2) \ln (p(v_1)p(v_2)) dv_1 dv_2 = \\ &= - \int p(v_1)p(v_2) \ln p(v_1) dv_1 dv_2 - \int p(v_1)p(v_2) \ln p(v_2) dv_1 dv_2 = \\ &= - \int p(v_1) \ln p(v_1) dv_1 - \int p(v_2) \ln p(v_2) dv_2 = H(v_1) + H(v_2) \end{aligned} \quad (3.11)$$

It has been demonstrated that the mutual information of variables with unitary variance is equal to the negentropy less than the sign and a constant and that the minimization of the mutual information coincides with the maximization of the negentropy.

Maximum likelihood estimation

Independent components can be estimated through the maximization of the log-similarity function defined as

$$L = \sum_{t=1}^T \sum_{i=1}^n \log p_i[(w_i^T \mathbf{x}(t))] + T \log |\det \mathbf{W}| \quad (3.12)$$

where T is the duration of the time series, w_i is the i^{th} row of matrix \mathbf{W} and p_i is the probability density of the i^{th} source signal.

3.3.4 Limitations and advantages of ICA

The main limitation in the application of ICA, as explained above, is that Gaussian sources cannot be separated even if they are independent. Partitioning with ICA can be done only if at most one source in the mixture has a Gaussian distribution. In fact, if all sources have a Gaussian distribution, any linear combination of them still has a Gaussian distribution, so it is impossible to separate them trying to make them non-Gaussian. [14]

This method has other inherent limitations. First, it can decompose, at maximum, N sources from N data channels. The exact number of statistically independent signals that contribute to scalp EEG is generally unknown, but brain activity is probably derived from sources that are actually more physically separable than the number of EEG electrodes available. Secondly, ICA is based on statistical analysis of data, so its results will not be significant if the amount of data provided to the algorithm is insufficient. In general, it is best to use all available data to reliably derive the spatial filters that characterize the appearance and spread of artifacts in the EEG. However, this is only true when the physical sources of artifact and brain activity are spatially stationary over time and the total number of these sources is less than the number of data channels. Overall, there is no reason to believe that brain sources and artifacts are spatially stationary over time. The goal should therefore be to use the maximum amount of data during which the sources are reasonably stationary.

Despite the not few limitations, the analysis of independent components has several advantages. [21] The algorithm is computationally efficient and the calculation demands are not excessive even for fairly large EEG data sets. Another benefit of this technique is that it is generally applicable for the removal of a wide variety of EEG artifacts. It simultaneously separates both the EEG and its artifacts into independent components based on data statistics, without relying on the availability of one or more "clean" reference channels for each type of artifact. In addition, separate analysis is not necessary to remove the different classes of artifact. Once the training is completed, artifact-free EEG records can then be obtained in all channels by simultaneously removing contributions from various artifact sources identified in the EEG record. [22]

3.4 ICA Decomposition

The following ICA-based algorithms have been evaluated: Infomax, fastICA and robustICA. The three algorithms are available in EEGLAB [23], an open source toolbox that provides a graphical user interface and integrated functions that can be easily integrated into custom Matlab scripts.

EEGLAB allows the user to read data, information on events and channel detection files in different formats, including Matlab and Biosemi EDF. EEGLAB's standard data analysis functions include filtering of data, extraction of data epochs, database removal, reference average conversion, resampling of data and extraction of time-locked data epochs to specific experimental events. EEGLAB also includes methods that allow users to remove entire channels of data, eras or components dominated by non-neural artifacts through visual inspection.

The figure 3.4 below shows the typical user interface related to the properties of the single independent component. In particular it is shown, on top left there is the topographic 2-D scalp map, on top right there is the plot of the event-related potential, ERP, on the bottom there is the representation of the power spectrum activity. Through the commands below there is the possibility to accept or reject that component, after having an overall view of the IC properties.

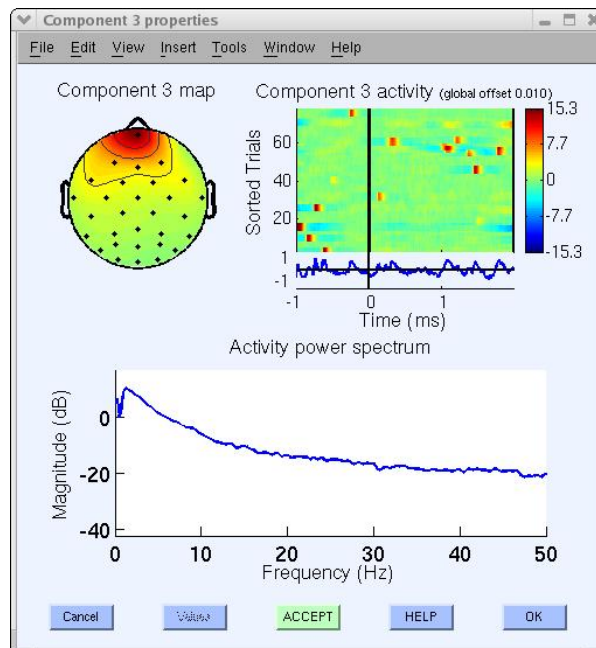


Figure 3.4. *Component Properties for a single IC in EEGLAB*

3.4.1 Decomposition algorithms

Below is a brief description of the theoretical principle behind these methods, without going into the details of the optimization algorithms used:

- Infomax: This algorithm is based on maximizing mutual information between the input and output of a neural network. The method minimizes mutual information between sources. [24] This particular algorithm works on bleached data and is easy to implement for the search of independent components.
- FastICA: This algorithm minimizes gaussianity through a measurement of negentropy. [18]
- RobustICA: This algorithm uses a kurtosis contrast function. [25]

The last two algorithms are based on gaussianity measurements. The central limit theorem provides a justification for using the technique of non-gaussianity maximization for the estimation of independent components, IC. This theorem asserts that the linear combination of k independent random variables converges to a Gaussian distribution as k increases whatever the probability density function of the individual variables. According to this theorem, if the independent variables that are combined are non-Gaussian, as assumed to be the sources of the ICA model, then their linear combination is certainly more Gaussian than the individual independent variables.

Chapter 4

Cross-frequency coupling

In more and more studies, the human brain is being shaped as a complex network with distributed topology. All this can be translated into parallel, specialised information processing.

Therefore, the need to elaborate a neural mechanism that allows the integration of information through specialised brain regions has arisen. [26]

What has emerged from recent studies is that oscillations from different frequency bands are not isolated and independent; consequently, they can interact with each other in the form of modulation.

The study of interactions between different oscillations at various frequency bands is called cross-frequency coupling, CFC. Different couplings have been studied, including phase-amplitude, phase-phase and amplitude-amplitude.

Phase-Amplitude Coupling, PAC, is the most studied type of cross-frequency coupling and is believed to be responsible for the integration of neuron populations. In particular, with PAC the phase of the lower frequency oscillation drives the amplitude of the coupled upper frequency oscillation, which results in the synchronization of the amplitude envelope in faster rhythms with the phase in slower rhythms.

Cross-frequency coupling could prove to be a mechanism underlying the coordination of neural dynamics. Several research groups have studied CFC and linked it to information processing, in particular learning and memory. It has also been shown that the study of CFC to study neurological and psychiatric disorders. Thus, CFC analysis is potentially a promising approach to reveal brain functions and some of their pathologies.

In particular, the PAC has aroused growing interest, given the growing amount of evidence of its potential role in processing information about the brain and its changes in pathological conditions, including epilepsy.

Within the PAC the instantaneous amplitude of a higher frequency band within a signal is modulated by the instantaneous phase of a lower frequency band within the same signal.

4.1 Feature extraction steps

Several studies in the literature on the electrophysiology measurement of neural activity have observed that different frequency bands are responsible for distinct computational roles, as the oscillations create synchronisations between specialised regions to ensure cognitive processing. [27]

CFC is not limited to memory processes, but has been reported in sensory processing, including vision and visual attention, smell, and auditory perception. For example, as mentioned in the previous chapter, neuronal activity of the gamma band in the human brain has been shown to play an important role in visual perception, while fluctuations in the alpha band in the occipital region have been interpreted as an indicator of reduced visual attention.

To proceed with the PAC calculation, conventionally there are three steps to be completed:

1. filter the input data in the bands of interest, in our case, in alpha and gamma band
2. apply the Hilbert transform to extract the amplitude and phase time series from each frequency band of interest
3. quantify the relationship between the phase and the time series of amplitude

The following will be explained in a little more detail.

4.1.1 Band component extractions

For the extraction of spectral components from a signal, filtering must be done first. For filters, there are two broad categories:

- Finite Impulsive Response - FIR: these filters are characterized by a finite, symmetrical pulse response and have a linear phase. These filters can be described through an MA system, Moving Average. If a linear phase filter is used, a shift is introduced in the signal and this time delay is proportional to the order of the filter and is the same for all harmonic components.
- Infinite Impulsive Response - IIR: these filters have an infinite impulsive response and a non-linear phase. They can be recursively defined with an ARMA, AutoRegressive Moving Average system. In this case, being the non-linear phase, the delay is different at different frequencies and this leads to a distortion of the signal. To avoid this, a null phase filtering must be used, so as to modify only the input module of the signal and not the phase.

4.1.2 Phase and amplitude extraction

In our study CFC represents the link between the alpha-band phase and the gamma-band amplitude, therefore it is necessary to extract these components from the signal to be analysed.

Hilbert's transform was used to obtain the phase and amplitude trend over time. This transformation can be interpreted as a function that receives an input vector x , the analytical signal, containing the real values of the signal to be analysed and returns a complex vector in output.

$$x_a(t) = x(t) + i\mathcal{H}(x(t)) \quad (4.1)$$

where $\mathcal{H}(x(t))$ is the Hilbert's transformation of $x(t)$ and i is the imaginary units. The output vector is composed of the real part x which is the same input vector x , while the imaginary part y is the vector x out of phase by 90° .

If the phase of the Hilbert transform of a signal is calculated, the phase trend over time is obtained. Therefore, to obtain the alpha band phase, the alpha band signal must be filtered, then apply the Hilbert transform and finally extract the phase. As far as the amplitude trend in time is concerned, instead, the transformation module must be determined. In our case, to obtain the amplitude in the gamma band, first filter the signal in the gamma band, then apply the transform and finally calculate its module.

4.2 Coupling Indexes

To obtain an idea of the level of coupling between phase and amplitude, numerical indexes can be used. There is no unique convention on how to calculate phase-amplitude coupling, but there is a heterogeneity of methods used in the literature.

Some of the most widely used phase amplitude coupling measurements today are phase locking value PLV, the mean vector length MVL, the modulation index MI, the GLM method of generalized linear modeling and phase binning combined with variance analysis ANOVA. Recent approaches use mutual information to calculate phase-amplitude coupling. The calculation of mutual information is sensitive to the amount of data and noise, but is advantageous when dealing with non-linear relationships. All these measurements use the instantaneous phase and amplitude of the signals after being filtered with a bandpass to calculate a measurement representing the coupling force. [28]

A first comparison between the indices in terms of noise level, coupling phase, data length, sampling frequency, non-stationary signal and multi-mode, showed that: the performance of the various indices differed considerably in conditions of poor quality of the analysed signal, including high noise and low sampling frequency, but all showed good qualities in the presence of signal with good qualities, such as

longer periods and less noise.

The main characteristics of the most used indexes in the literature are shown below.

Modulation Index - MI

The MI is an index that quantifies the deviation of the phase amplitude distribution from the uniform distribution through the Kullback-Leibler divergence. [29]

This index can change between 0 and 1, and is equal to 0 in the complete absence of coupling. To obtain a value approximately equal to 1, an amplitude function completely opposite to a uniform distribution should be used, i.e. a distribution that resembles the Dirac Delta.

Through experimental tests in literature, it has been seen that the MI index has very low values, about 10^{-3} 10^{-4} .

This index is robust when used in the presence of noise and even with short data ages.

Phase Locking Value - PLV

The phase locking value index is another method used for coupling measurement. In this case the PLV is calculated starting from the time trend of the alpha phase and the corresponding amplitudes in the gamma band.

Therefore it calculates the circular variance of the consistency of the phase differences between the low frequency signal phase and the high frequency signal amplitude phase.

We can speak of reciprocal modulation if the time course of the amplitudes in the gamma band are in phase with the alpha band waves. In this case the index tends to 1 if the difference between the phase and the amplitude of the two bands remains constant over time, and in this case we speak of phase locking. In the same way, the PLV value deviates from the unit value the more the difference between phase and amplitude changes over time.

Mean Vector Length - MVL

This index quantifies circular variances by the amplitude of the average of the complex composite signal. To obtain good results, this index requires the use of a signal characterised by high SNR.

This index is calculated as the modulus of the time average of the vector representing the graphical projection between phase and amplitude.

What is therefore studied is an estimate of the centre of the figure created by the projection on the complex plane of the vector. It has been analysed that in the absence of coupling, on the complex plane, the vector designs the circular figures centred in the origin as time varies. In fact, in the absence of coupling, the amplitude of the gamma waves are equally distributed in all the phases of the alpha

waves and the value of the MLV index tends to 0. If coupling is present, the centre of the graph will no longer be centred at the origin and the index deviates from the zero value the greater the coupling between phase and amplitude. [30]

From the calculation of this index there are three tricks: the final value depends on the general absolute amplitude of the amplitude providing the frequency, outliers can strongly influence the measurement and phase angles are often not uniformly distributed.

After a statistical comparison between the three indices described above, in which the focus was on the effects of data length and the accuracy of finding the coupling frequencies that contribute within exploratory analyses over wide frequency ranges, the following conclusions were reached. MVL estimates the coupling force more correctly and MI is more robust to noise with regard to the detection of coupling frequencies.

4.3 CFC and Neural Disorder

Several studies that process information received from the cerebral cortex have hypothesized that high frequency brain oscillations reflect local cortical information processing and that low frequency brain oscillations project the flow of information through larger cortical networks.

The CFC refers to the link between two bands within the signal. In this work the link between the phase of the alpha band waves and the amplitude of the gamma band waves has been studied cause there are numerous studies in the literature that have studied their application to cases of epileptic patients.

This type of coupling has aroused a lot of interest over the years as it is considered fundamental for the correct functioning of the memory, both sensorial and associative. [27] Moreover, given the close link with remembering, its study could play an important role in research on neuro-degenerative diseases.

PAC can be studied for the functional aspect of normal brain dynamics, and in the same way the study of an abnormal PAC could be a cause or symptom of unhealthy brain function. Several studies have worked on the PAC applying it between different frequency bands, in different brain regions and under different working conditions. Associations between brain disease and PAC have been found in epilepsy, Parkinson's disease, Alzheimer's disease. This makes the PAC estimate of interest for clinical trials.

Over the years, the idea that there may be a scientific and clinical basis for investigating the role of CFCs in healthy patients and patients with neurological disorders has been growing. In particular, as already mentioned, more and more attention has been focused on the study of the PAC, as it has been widely demonstrated that several neurological diseases can alter its characteristics due to its rhythmic activity. [31]

Neural mechanism of CFC

Although CFC has been widely studied, its neurophysiological relevance has never been fully understood and is still under study. A number of theories have been hypothesized that link some computational models to the data recorded in human and animal studies.

A modulation study has demonstrated a series of fundamental properties necessary for a brain network to generate CFCs: first of all, it is necessary to be in the presence of distinct multi-frequency neural oscillations and also to have different coupling mechanisms between the single neuronal circuits responsible for rhythmic activities. The first property is based on synaptic coupling between excitatory and inhibitory populations and also, electrical coupling between individual neurons through gap junctions.

In this thesis work the coupling between the low frequency alpha phase and the high frequency gamma amplitude was analysed. It has been seen in some studies how gamma activities may result from interactions within highly interconnected inhibitory neuron populations or may result from network interactions between exciting local interneuron network populations. For alpha band oscillation activity, however, these are the result of the interneuronal network activity involving both pyramid cells and interneurons and their interactions in generating a range of oscillations.

There has also been an in-depth study in the literature on the effect that certain neurotransmitters may have on CFCs. In a recent study, the effects of dopamine release on CFC modulation between different frequency bands were explored in a study population consisting of rats that have been given dopamine.

Chapter 5

Results and Discussions

5.1 Dataset

The dataset consists of fifteen patients with EMA, eyelids myoclonia with absences, a disease that will be described in the next paragraph.

Specifically, there are thirteen females with an average age of 25.4 years and an average age of onset of epilepsy at 8 years. The demographic and electro-clinical details of the EMA group are summarized in the following Table 5.1.

The inclusion criteria for the diagnosis of EMA were as follows:

1. age of onset between 2 and 14 years
2. eyelid myoclonus with or without absence
3. related generalised paroxysmal activity
4. epileptic seizures induced by eye closure, electroencephalographic paroxysms (EEG) or both, within 0.5-4 seconds of eye closure
5. photosensitivity

Scalp EEG was recorded by means of a 32-channel MRI-compatible EEG recording system (Micromed, Treviso, Italia).

Simultaneously, a video was recorded during the EEG-fMRI acquisition, which made it possible to control the movements and physiological activities of the patients and controls, as well as the eyelid myoclonus triggered by the closing of the eyes in the EMA.[32] For part of the work, the video was essential to recognise the exact moment of eye closure.

5.1. DATASET

Patient	Age Seizure Onset	Sex	Cognitive Status	Voluntary Eye Closures	Spontaneous Blinks
1	16/8	M	Normal	12	91
2	29/8	F	Normal	21	39
3	18/5	F	Normal	12	91
4	21/9	F	Mind mental retardation	13	191
5	21/13	F	Learning disability	12	12
6	17/11	M	Normal	12	35
7	26/9	F	Normal	12	46
8	30/15	F	Normal	12	42
9	18/13	F	Normal	12	21
10	56/14	F	Normal	12	70
11	35/14	F	Normal	12	3
12	19/2	F	Learning disability	12	29
13	57/NR	F	Normal	12	85
14	11/9	F	Normal	12	64
15	8/5	F	Learning disability	13	36

Table 5.1. Demographic and Eletroclinical Features of Patients with EMA

Patients were trained to open and close their eyes for periods of 30 seconds in response to a beep from a headset. Each condition was repeated 3 times per session for 4 consecutive sessions lasting 3 minutes, so a total of 12 conditions with eyes closed and eyes open. The first and third fMRI series started with eyes closed, the second and fourth with eyes open. This sequence was alternated from one subject to another. [33]

5.1.1 Eyelid myoclonia with absences

The International League against Epilepsy, ILAE, proposal Diagnostic Scheme of Epileptic Seizures has recognized eyelid myoclonia as a seizure type, but EMA is not one of the epilepsy syndromes, blending it with other photosensitive epilepsies under the etiquette of other visually sensitive epilepsies.

Jeavons in 1977 [34] for the first time gave a complete description of epileptic syndrome characterised by eyelid myoclonus associated with brief absences and photosensitivity, i.e. eyelid myoclonia with absences, EMA.

Eyelid myoclonia, not absences, is the hallmark of Jeavons syndrome. Eyelid myoclonia consists of a marked tearing of the eyelids often associated with an upward jerking deflection of the eyeballs and retropulsion of the head. This may be associated with or followed by a slight impairment of consciousness, precisely eyelid myoclonia with absences.

Seizures are short, usually lasting 3-6 s and occur mainly and immediately after closing the eyes and repeatedly many times a day. All patients suffering from this pathology are photosensitive. Myoclonic shots of the limbs may occur, but they are rare and random. The onset is typically in childhood with a peak at the age of 6-8 years.

From a pharmacological point of view, modern therapeutic combinations, such as valproic acid and ethoxymide, or valproic acid and lamotrigine, are usually effective; however, in a percentage of patients, seizures are resistant to pharmacological treatment.

5.2 Ocular Artifact Removal

The EOG waveform depends on the direction of eye movement. The vertical movement of the eyes produces a square waveform while the blink of the eyelashes looks like a waveform with a very intense peak, with a duration of about 0.2-0.4 s.

As already mentioned in the previous chapter, these types of artifacts are usually eliminated by regression methods that require EOG recording.

The method used in this work for the removal of artifacts has been proposed and implemented on the EEGLAB Matlab toolbox by German Gomez-Herrero [35], it is a fully automatic method based on the fastICA algorithm that does not require the EOG tracks.

The technique used can be divided into three basic steps [36]:

1. FastICA algorithm application and source estimation. Starting from equation 3.2, it is possible to write:

$$\mathbf{x}(t) = \mathbf{x}_{EEG}(t) + \mathbf{x}_{EOG}(t) = \mathbf{A}(t)\mathbf{s}(t) = \mathbf{A}_{EEG}\mathbf{s}_{EEG}(t) + \mathbf{A}_{EOG}\mathbf{s}_{EOG}(t) \quad (5.1)$$

where \mathbf{A}_{EEG} and \mathbf{A}_{EOG} are the submatrices of \mathbf{A} built considering only the columns of \mathbf{A} associated, respectively, to the neural and artifact sources, while \mathbf{s}_{EEG} and \mathbf{s}_{EOG} indicate the neural and artifact sources.

2. Identification of artefact sources. It has been chosen to use a criterion based on fractal dimension, FD, for the determination of the sources associated to artefact components.

FD is a measure of signal complexity, in fact the EOG spectrum presents a dominance of low frequency components while the EEG spectrum is more distributed and flatter. For these reasons neural sources have higher FD values than those related to eye activity.

In particular, the Sevcik algorithm is used to calculate FD, which maps the waveforms in a unitary square to create standardised coordinates.

The fractal dimension is calculated as follows:

$$FD = 1 + \frac{\ln(l)}{\ln(2(n-1))} \quad (5.2)$$

where l is the total length of the waveform in the unitary square and n is the number of the points of the waveform.

To obtain a more robust estimate of the FD it is possible to divide the sources into windows containing 10% of the total samples, calculate the FD for each window and average them to obtain the FD_{mean} value. Sorting the sources according to their FD_{mean} in descending order, the \mathbf{s}_{EEG} will be the k sources s_1, s_2, \dots, s_k where k is the smallest integer in the range $M/2 \geq k \geq 1$ such that

$$(fd_{k+1} - fd_k) < (fd_k - fd_{k-1})$$

3. Removal of artifact sources and reconstruction of EEG data. After estimating the mixing matrix we can proceed with the reconstruction of the EEG signal of the various channels, multiplying the signals themselves with the sub-matrix \mathbf{A} and its pseudo-inverse \mathbf{A}^* .

$$x_{new}(t) = \mathbf{A}_{EEG}\mathbf{A}_{EEG}^*x(t) \quad (5.3)$$

These three steps described above are the steps applied to patients' EEG signals for EOG artifact removal. This algorithm was not applied directly to the entire signal but a time window was used without overlapping samples. This choice was made considering that the EEG signal is a non-stationary signal. For the time choice different tests were carried out and in the end a 200 s window was chosen which is the best to avoid an excessive removal of neural sources.

The figure 5.1 shows a complete EEG trace of a patient composing our dataset. In this case the patient was asked to open and close his eyes in response to a stimulus.

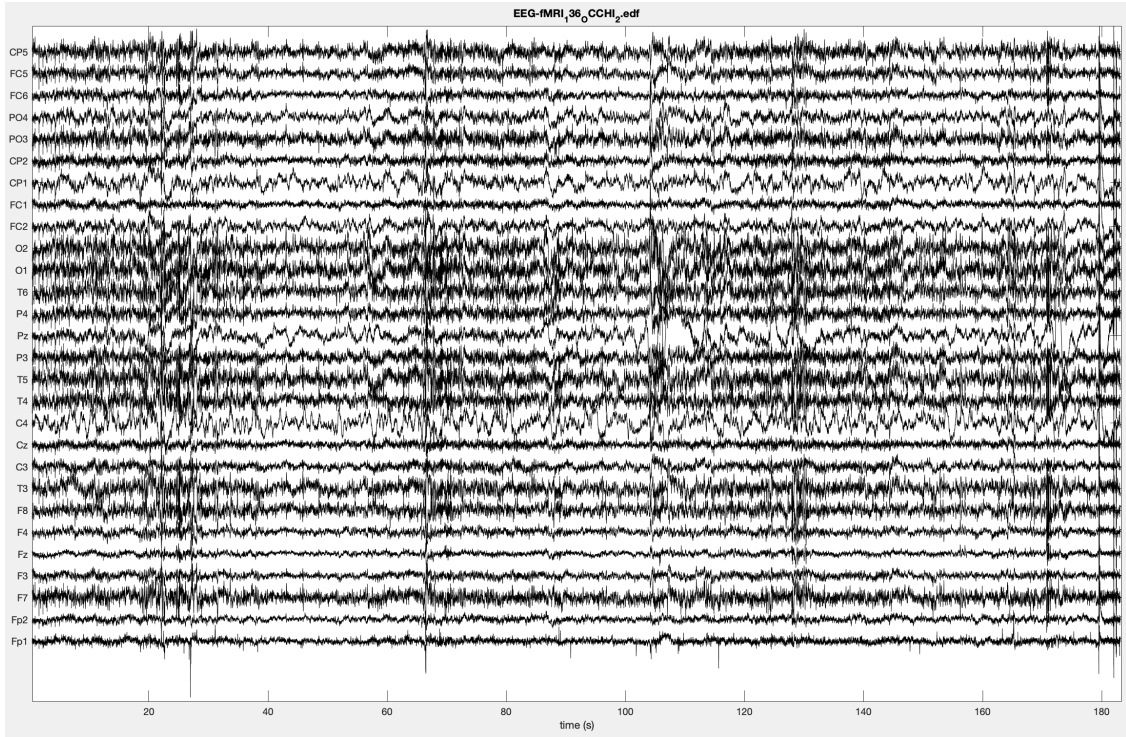


Figure 5.1. *Example of an EEG plotting*

Below are two excerpts from the epochs, of the signal shown above, with a length of 20 s to view the removal of artifacts in detail.

5.2. OCULAR ARTIFACT REMOVAL

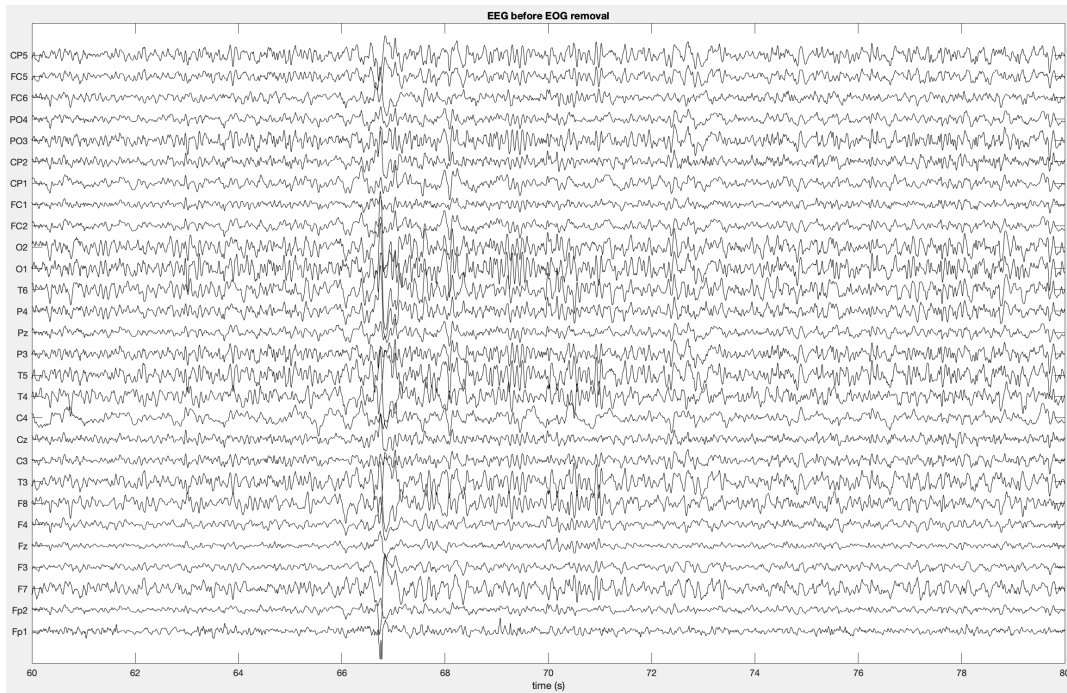


Figure 5.2. *Extract of an epoch 20s long before removal of the eye artifact*

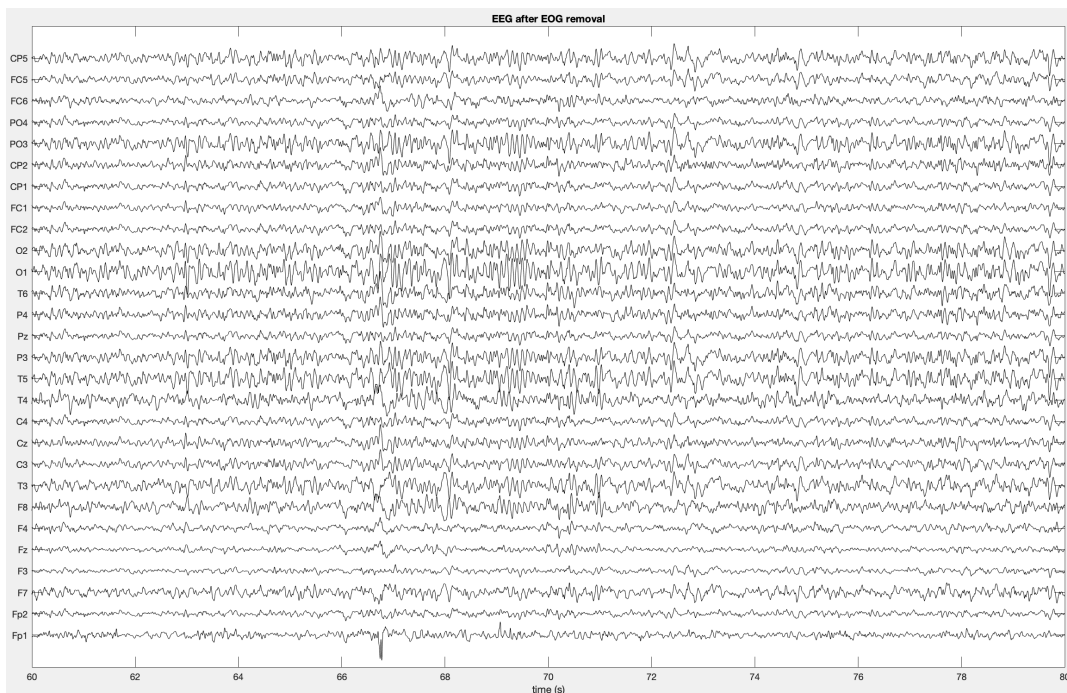


Figure 5.3. *The same epoch after removal of the eye artifact*

5.3 Cross-frequency coupling

To calculate the cross-frequency coupling, the phase of the filtered signal and the amplitude of the signal in each of the frequencies that compose the EEG signal have been calculated. In particular, after a study in the literature, it was decided to keep the electrode fixed in the occipital position and this was coupled with the other electrodes. Among all the indexes described, it was decided to use the PLV value to quantify the coupling between the various electrodes. The mathematical structure at the base of this index will be described below.

The algorithm elaborated for the calculation of the index has not been applied to the entire signal in its length, but has been divided into 3 second periods. These periods correspond to the event immediately after the closing or opening of the eye following an external stimulus. In the following these events will be called with the acronym *OA* to indicate the moment of the opening of the eye and *OC* to indicate the closing.

A further subdivision has been made to check whether or not the subject had an attack as a result of the stimulation. Again, acronyms will be used, specifically *pos* if there is a seizure or *neg* if it has not occurred.

To study the coupling, two indices were evaluated, in particular a bivariate index, the phase locking value, and an amplitude phase coupling indicator.

The graphs relating to a single patient are shown below, dividing the study by the different frequency bands and evaluating five different cases:

- epoch of length equal to 3s following the closure of eyes after an external stimulation and with the appearance of a seizure
- epoch of length equal to 3s following the closure of eyes after an external stimulation without the appearance of a seizure
- epoch of length equal to 3s following the opening of eyes after an external stimulation without the appearance of a seizure
- epoch of length equal to 3s taken at a random point while the subject had his eyes closed
- epoch of length equal to 3s taken at a random point while the subject had his eyes opened

Then the graphs for each brain rhythm will be shown for the two indexes studied. For each of them there are five graphs related to the five cases described.

5.3.1 Phase Locking Value - PLV

As already mentioned in the previous chapter, the Phase Locking Value is another index used for the mathematical measurement of coupling. In this case the index is calculated starting from the time trend of the alpha wave phase x_p and the corresponding amplitudes in the gamma band x_A . The idea behind the PLV is to compare the x_p vector with the alpha band phase of the x_A vector.

The first step is to filter the x_A signal into the alpha band and thus obtain the $x_{A\theta}$ vector. Then the temporal trend of the signal phase $x_{A\theta}$ will have to be extracted, going to calculate the phase of its Hilbert transform.

In mathematical formulas, this translates into:

$$y_{Ap} = \mathcal{L}hilbert(y_{A\theta}) \quad (5.4)$$

Then the vector x_p and x_{Ap} are compared with each other using the vector plv . This vector for each instant of time contains a complex number whose module is unitary and the phase is calculated as the instantaneous difference between the vector x_p and x_{Ap} .

$$plv(t) = e^{i[x_p(t) - x_{Ap}(t)]} \quad (5.5)$$

The PLV index is obtained from the average of the plv vector.

$$PLV = |\mathit{mean}\{plv\}| \quad (5.6)$$

This index will tend to 1 if the difference between x_p and x_{Ap} remains constant over time, and this is called phase locking. Instead, the PLV deviates from the unit value the more the difference between x_p and x_{Ap} changes over time.

Remembering how the dataset was structured, for each patient the recorded data showed repeated tasks carried out by the latter, such as the opening and closing of the eyes following a stimulus. The considerations that will be made for the PLV index and the PAC index, were made following several tests.

In fact, different positions indicating the same case were considered for the same rhythm. For example, 2 to 4 events were available for the study of the case of eye closure with a subsequent seizure within the track, so the results were elaborated for each of them and then general considerations were drawn.

For the graphic illustration of this index, the representation of the cerebral scalp was used. In particular, the 10 highest of the calculated couplings are highlighted within this index.

Note that we have chosen to keep an occipital electrode fixed because it is the one that is always more coupled and useful for the purpose of our study.

PLV index for delta rhythm

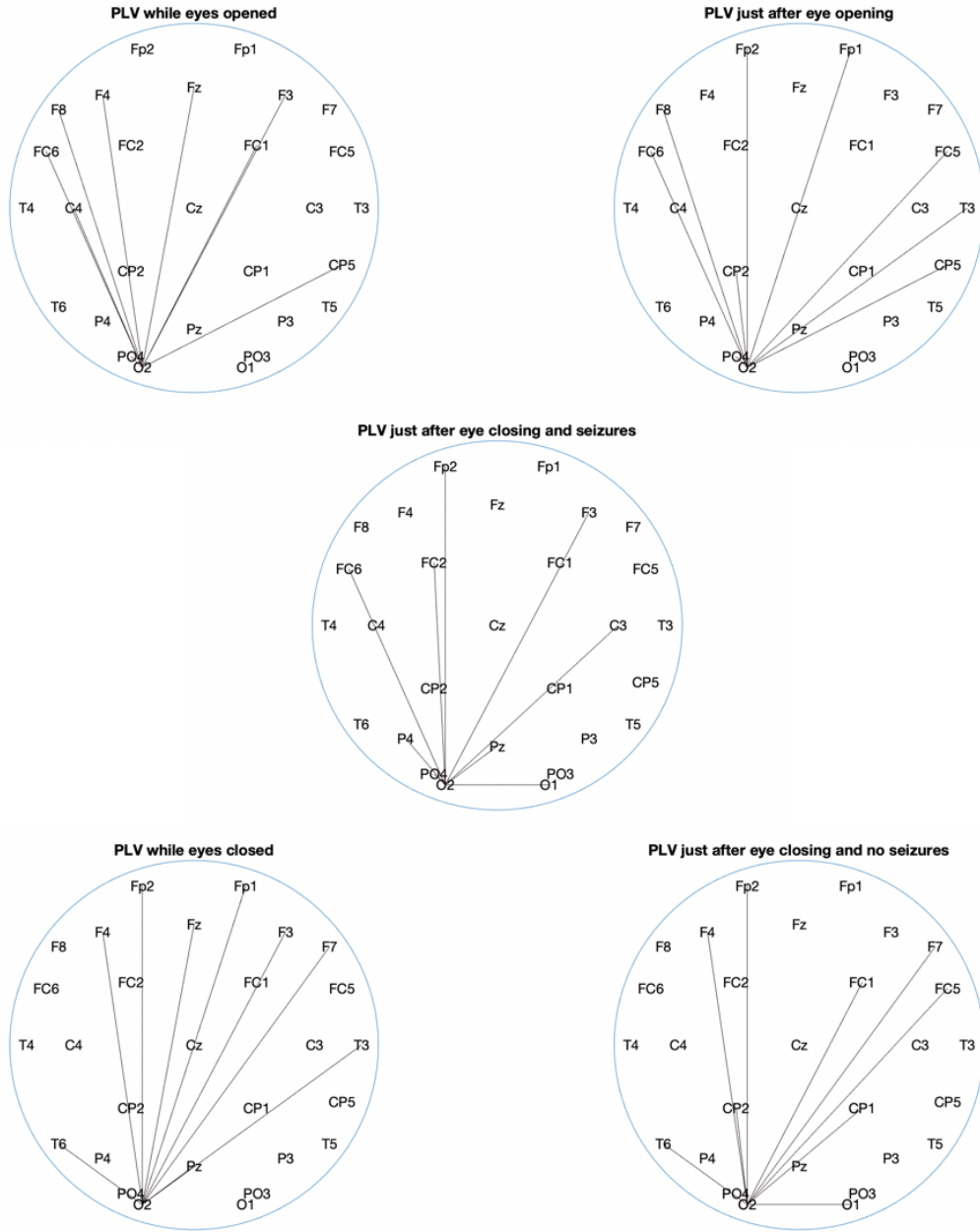


Figure 5.4. Representation of the 10 most paired electrodes in the delta rhythm divided in the five cases of clinical interest

By filtering the signals in the frequency range of the delta rhythm, it is possible to notice a greater coupling between the occipital electron and the frontal electrodes. The value of the average coupling represented is 0.09435.

PLV index for theta rhythm

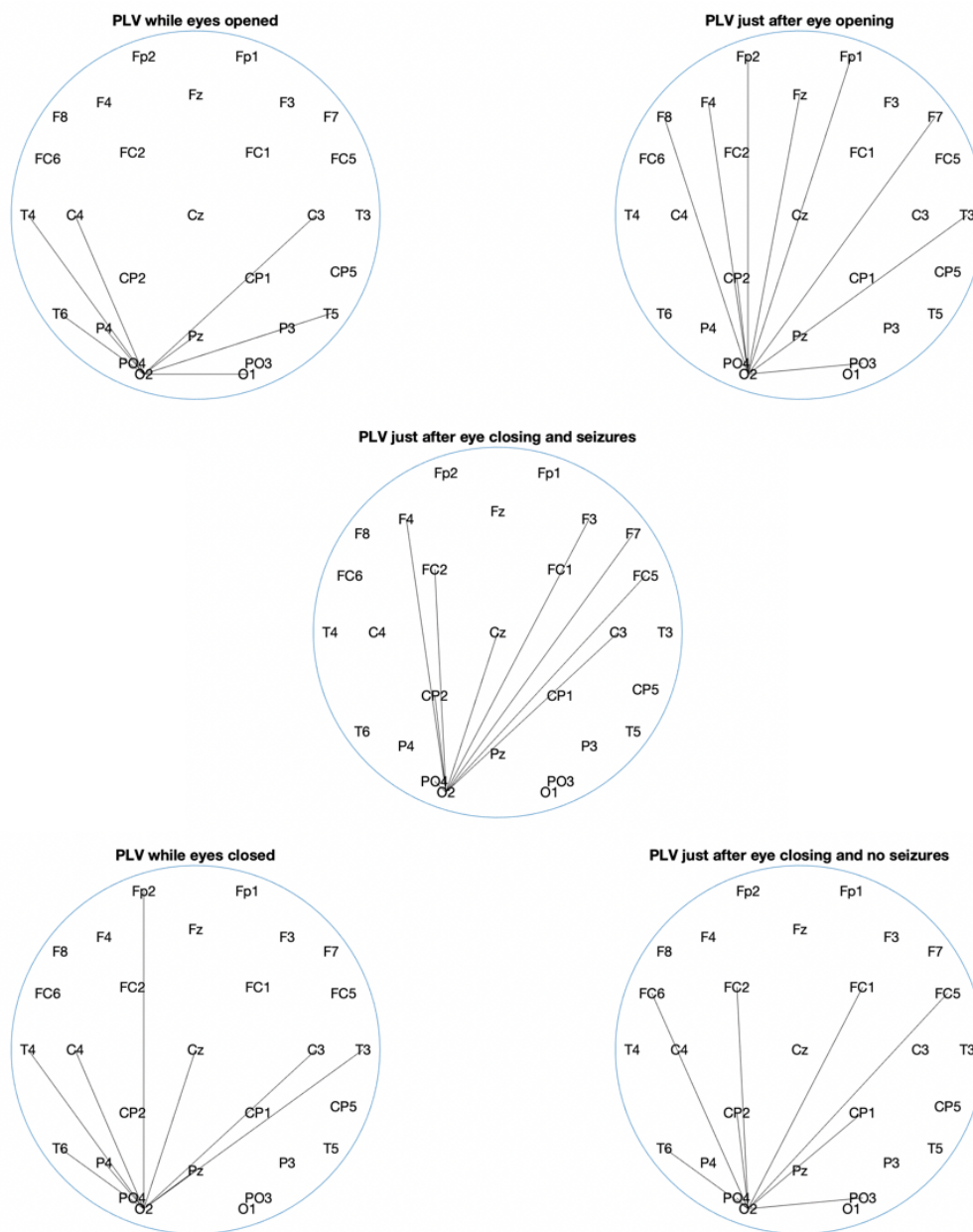


Figure 5.5. Representation of the 10 most paired electrodes in the theta rhythm divided in the five cases of clinical interest

For this particular case, after filtering the epochs with the theta frequency range, a greater coupling at central level has been noticed. In this case the average coupling value was 0.07632.

PLV index for alpha rhythm

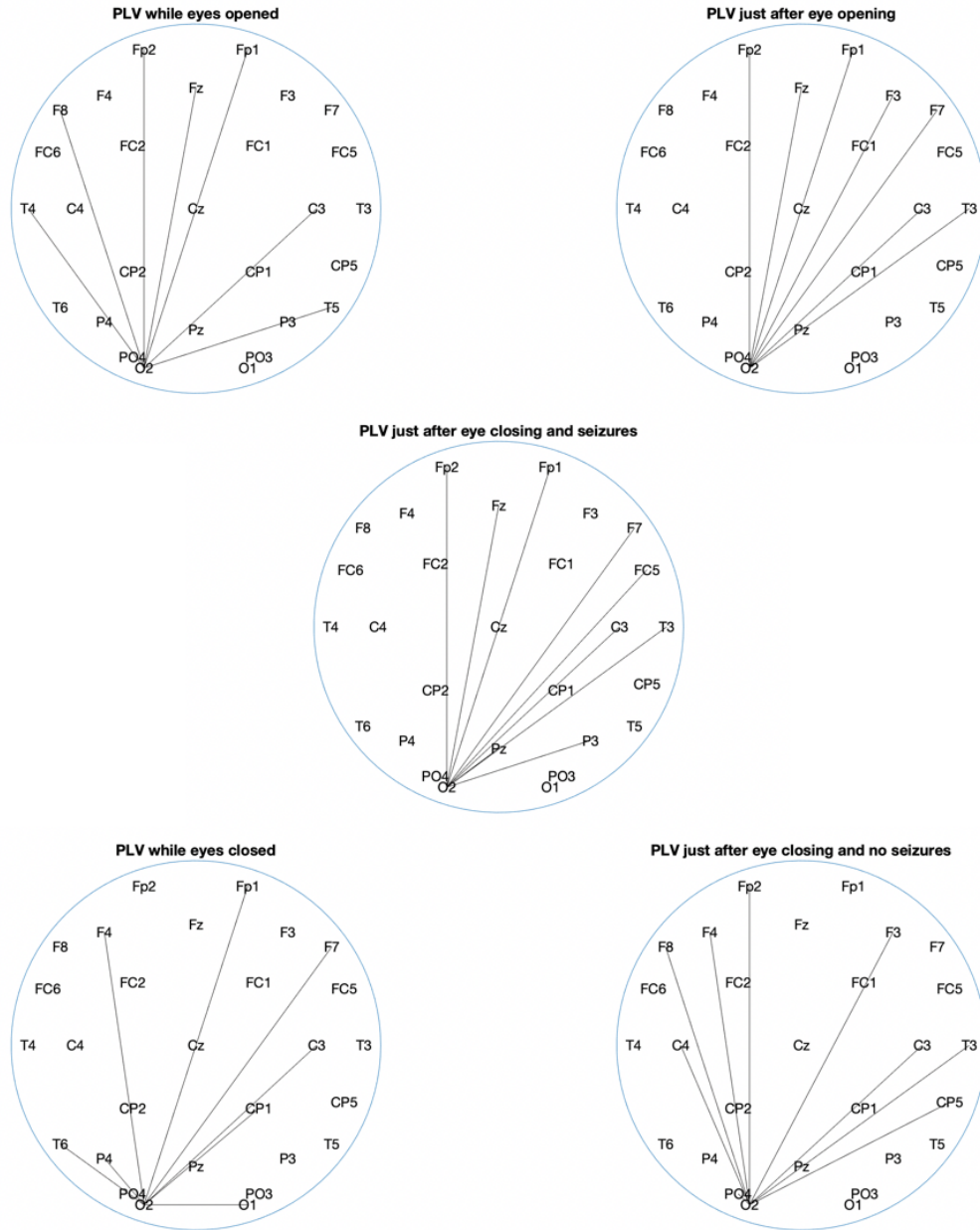


Figure 5.6. Representation of the 10 most paired electrodes in the alpha rhythm divided in the five cases of clinical interest

As in the case of delta-band filtering, there is greater coupling at the frontal level and in some cases, coupling at the temporo-occipital level has been noted. The average value for this patient in this range was 0.0657.

PLV index for beta rhythm

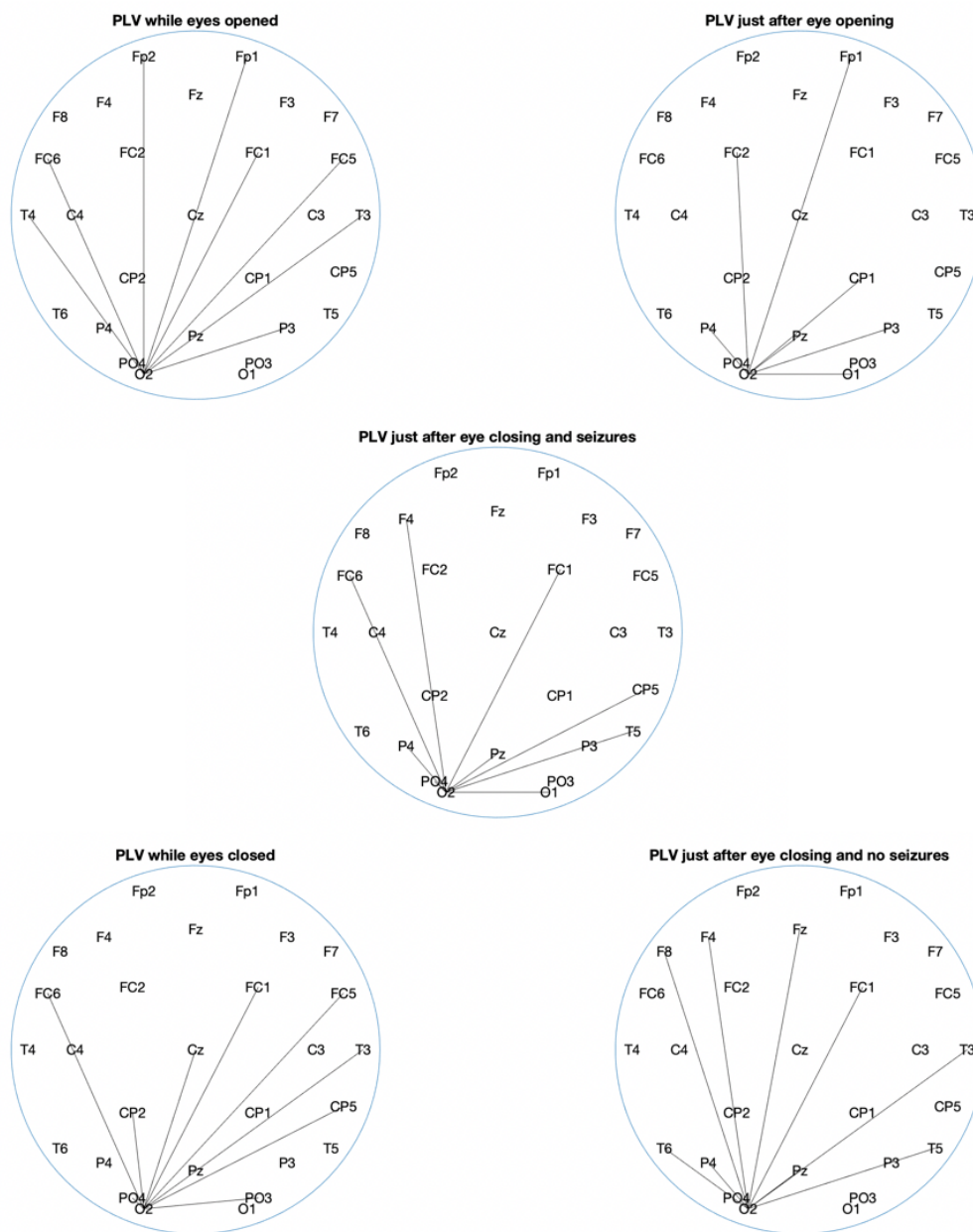


Figure 5.7. Representation of the 10 most paired electrodes in the beta rhythm divided in the five cases of clinical interest

In this case, a greater coupling has been noted at the front-central level. The average value calculated for the case of coupling in beta band was 0.0547.

PLV index for gamma rhythm

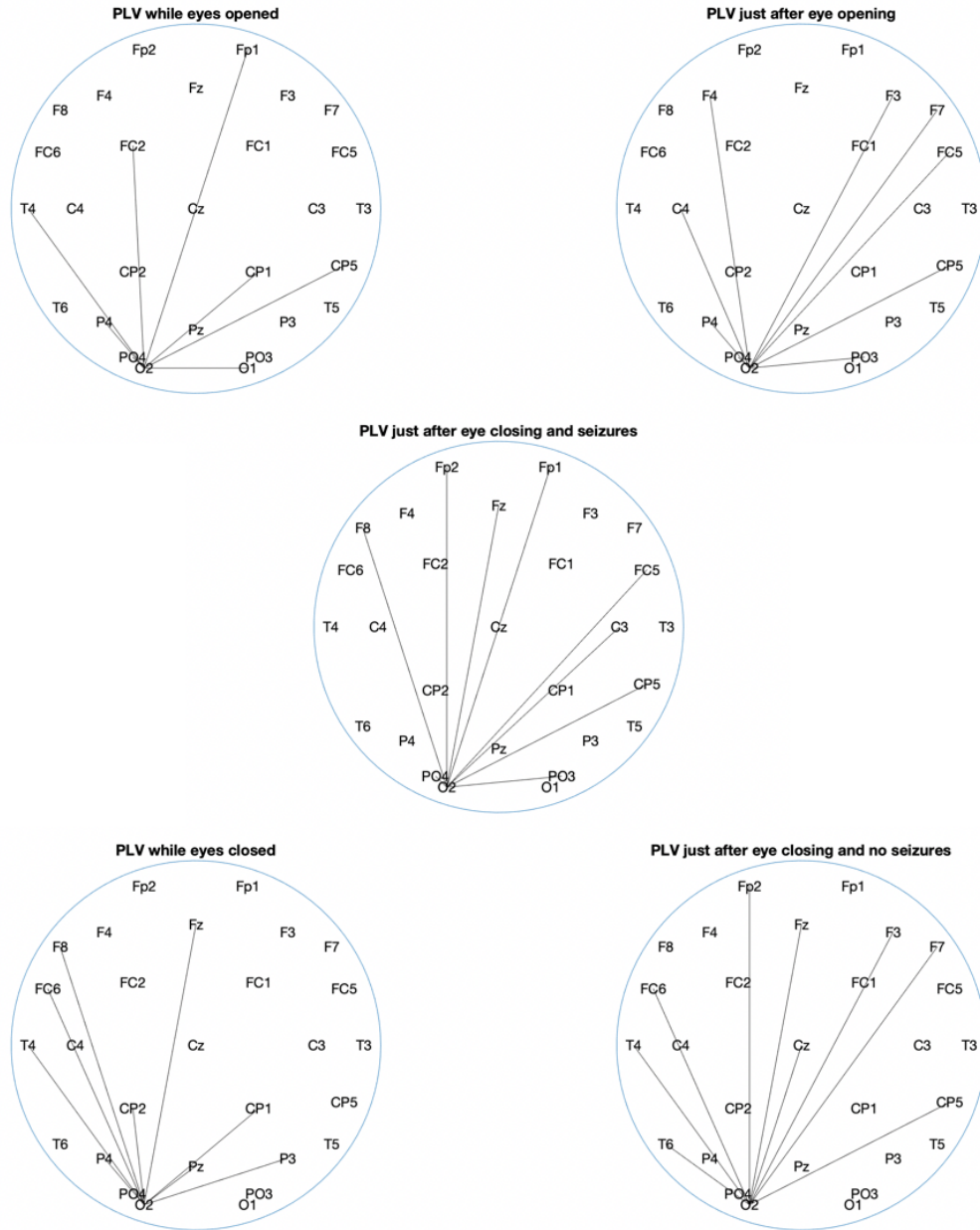


Figure 5.8. Representation of the 10 most paired electrodes in the gamma rhythm divided in the five cases of clinical interest

For the last frequency range analysed the results obtained were very variable between the various cases analysed even within the same run analysed. A very low average coupling value of 0.0234 is obtained.

After a comprehensive analysis of all patients, a general comparison can be made and common considerations can be drawn.

The first thing that was noticed is that the value of the PLV index decreases by increasing the frequency of study.

Another consideration that can be made for all cases is that the major couplings are almost always those between the occipital electrode and the frontal electrodes.

Subsequently, analogies were searched for similarities between the results obtained for the cases separately: for example, as expected, it was noted that during the eye opening and closing events there were higher coupling values between the occipital and frontal electrodes. For the events studied in random positions during which the patient's eyes were constantly closed or constantly open, on the other hand, no particular recurring characteristics were noted.

5.3.2 Phase Amplitude Coupling - PAC

Another index that has been calculated to numerically evaluate the coupling between the electrodes was the value R_{PAC} .

For its representation it was chosen to use a heatmap of the scalp shape. In particular, hot colours indicate higher index values and cold colours indicate lower values.

Also for this index will be shown for a single patient the five cases described in the previous paragraph separated for different brain rhythms.

For this index too, all events of the same type within the track have been subsequently considered for each event elaborated.

Making general considerations about coupling considering the same frequency band, there are some characteristics that distinguish some of them. For example, studies in the literature have shown that alpha-band coupling is mainly localised in the occipital and parietal regions and decreases towards the frontal area. This has often been found also in the cases studied in this work.

Another characteristic is on the study of the beta rhythm that is localized in the central-parietal regions and also this characteristic has often been noticed in this study.

PAC index for theta rhythm

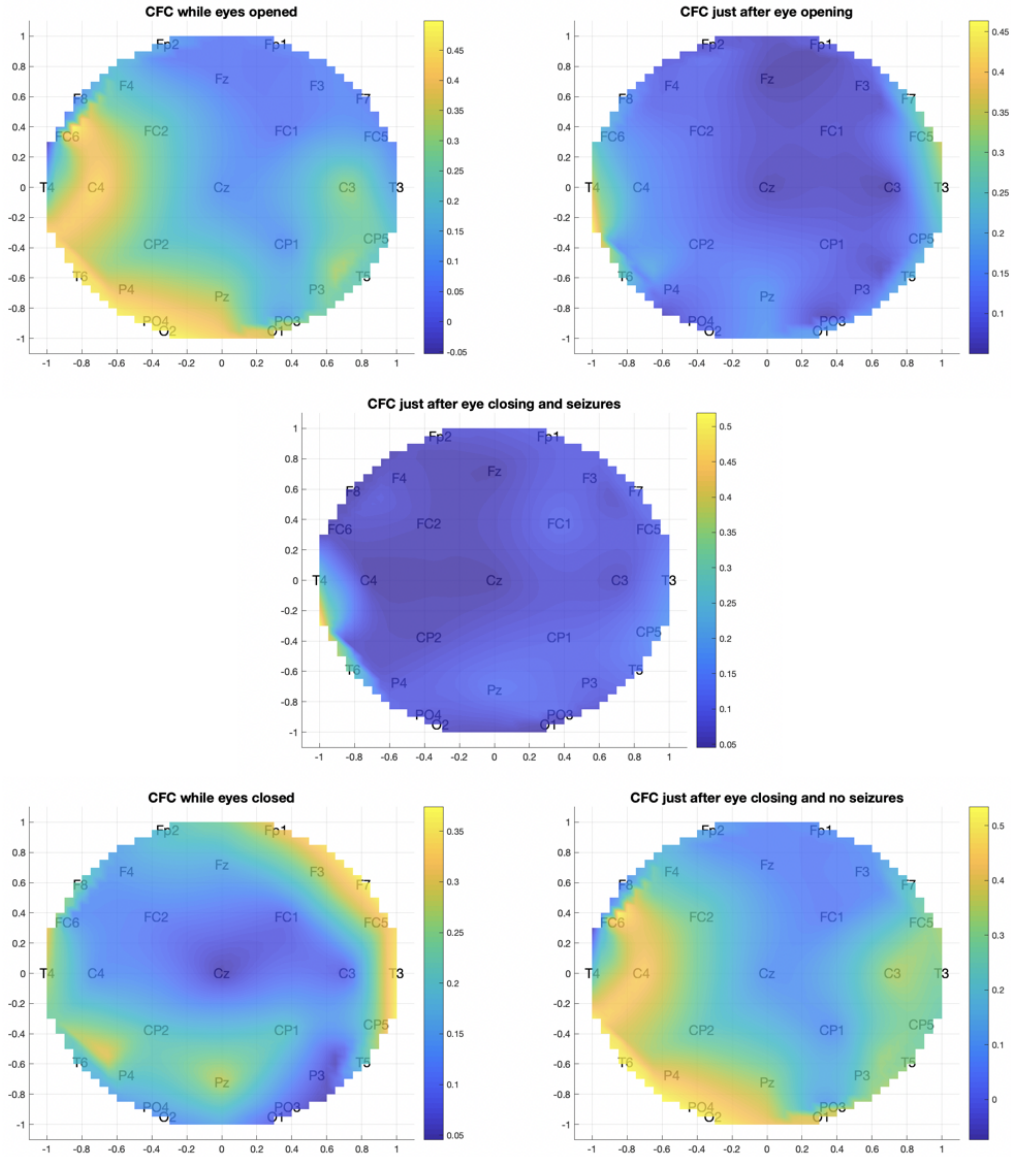


Figure 5.9. Representation of the heatmap to illustrate the PAC of the theta rhythm divided in the five cases of clinical interest

In this example it was possible to notice a coupling always present at the level of the temporal electrodes on the left side of the scalp. In one case, on the other hand, we have seen a high coupling at frontal level on the right side.

PAC index for alpha rhythm

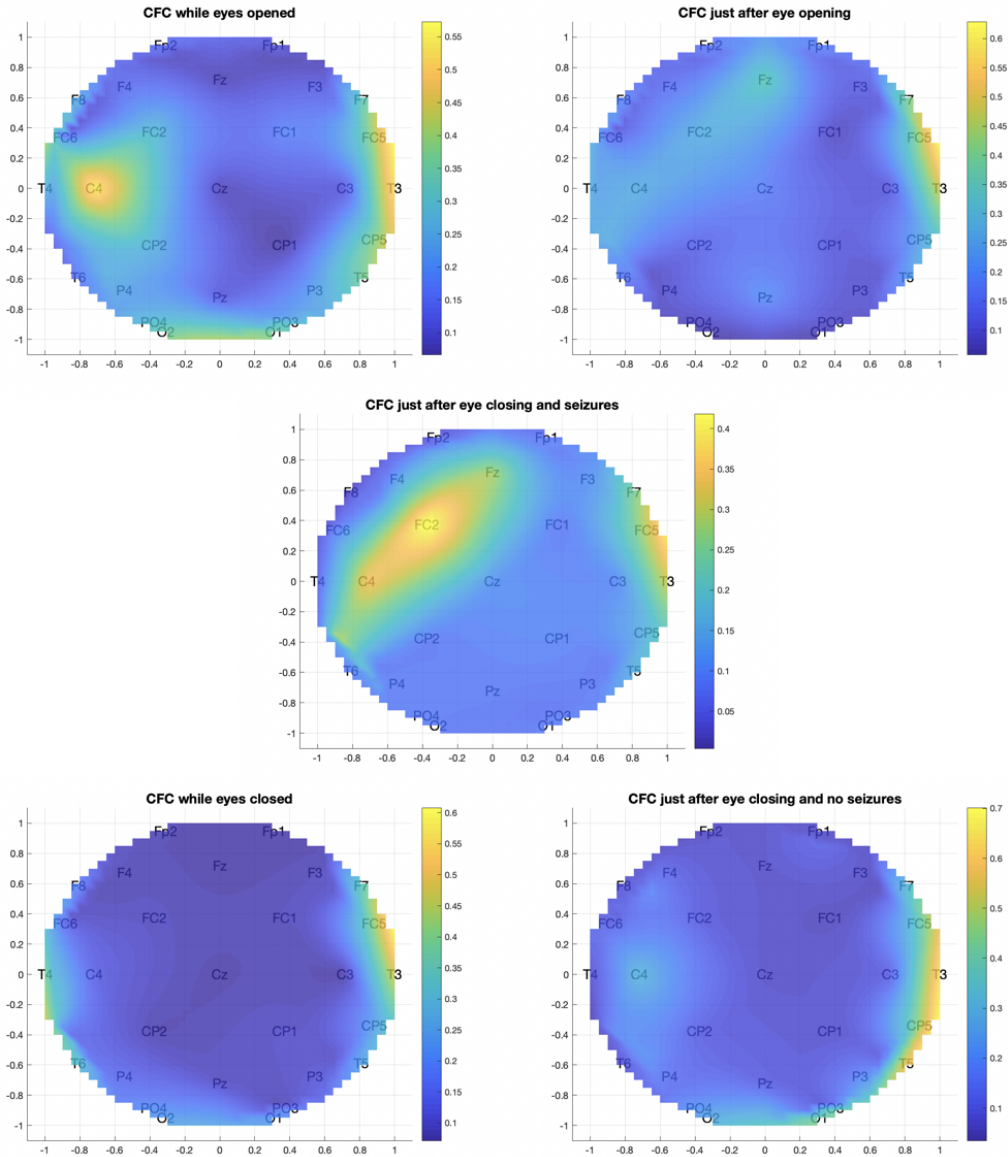


Figure 5.10. Representation of the heatmap to illustrate the PAC of the alpha rhythm divided in the five cases of clinical interest

In this example, when using alpha-band filtering, there is a greater coupling at the frontal-temporal level on the right side of the cervical. In the case of eye closure and a subsequent crisis it is possible to see a high coupling at the centre-frontal level.

PAC index for beta rhythm

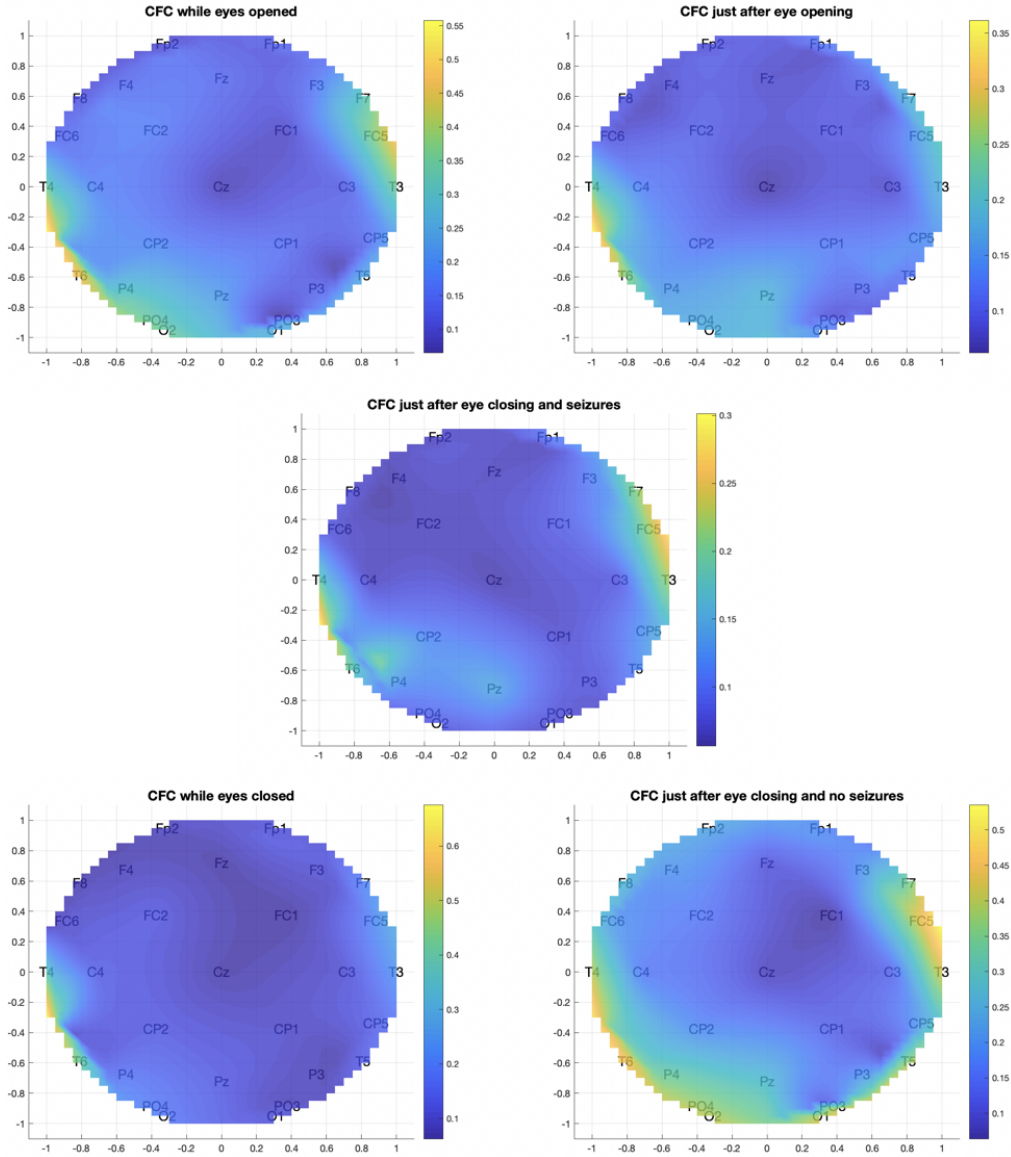


Figure 5.11. Representation of the heatmap to illustrate the PAC of the beta rhythm divided in the five cases of clinical interest

As far as the study of beta-band coupling is concerned, no particular recurrences are noted. This was also true for other patients.

PAC index for gamma rhythm

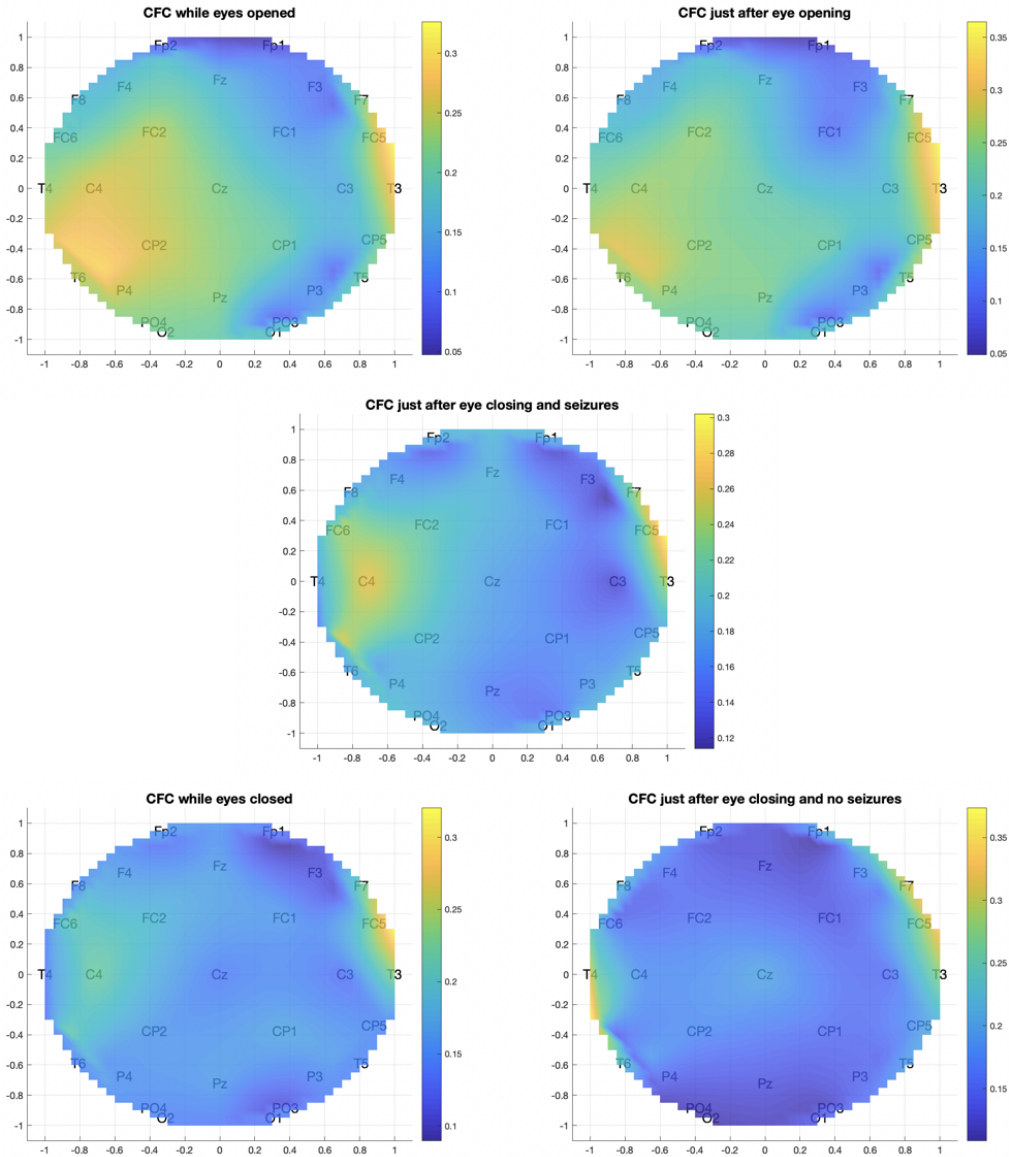


Figure 5.12. Representation of the heatmap to illustrate the PAC of the gamma rhythm divided in the five cases of clinical interest

In this case, the index value calculated by filtering the gamma band signal was the lowest. As you can see from the images in the figure, there is a higher coupling at the temporo-parietal level.

PAC index for alpha-gamma rhythms

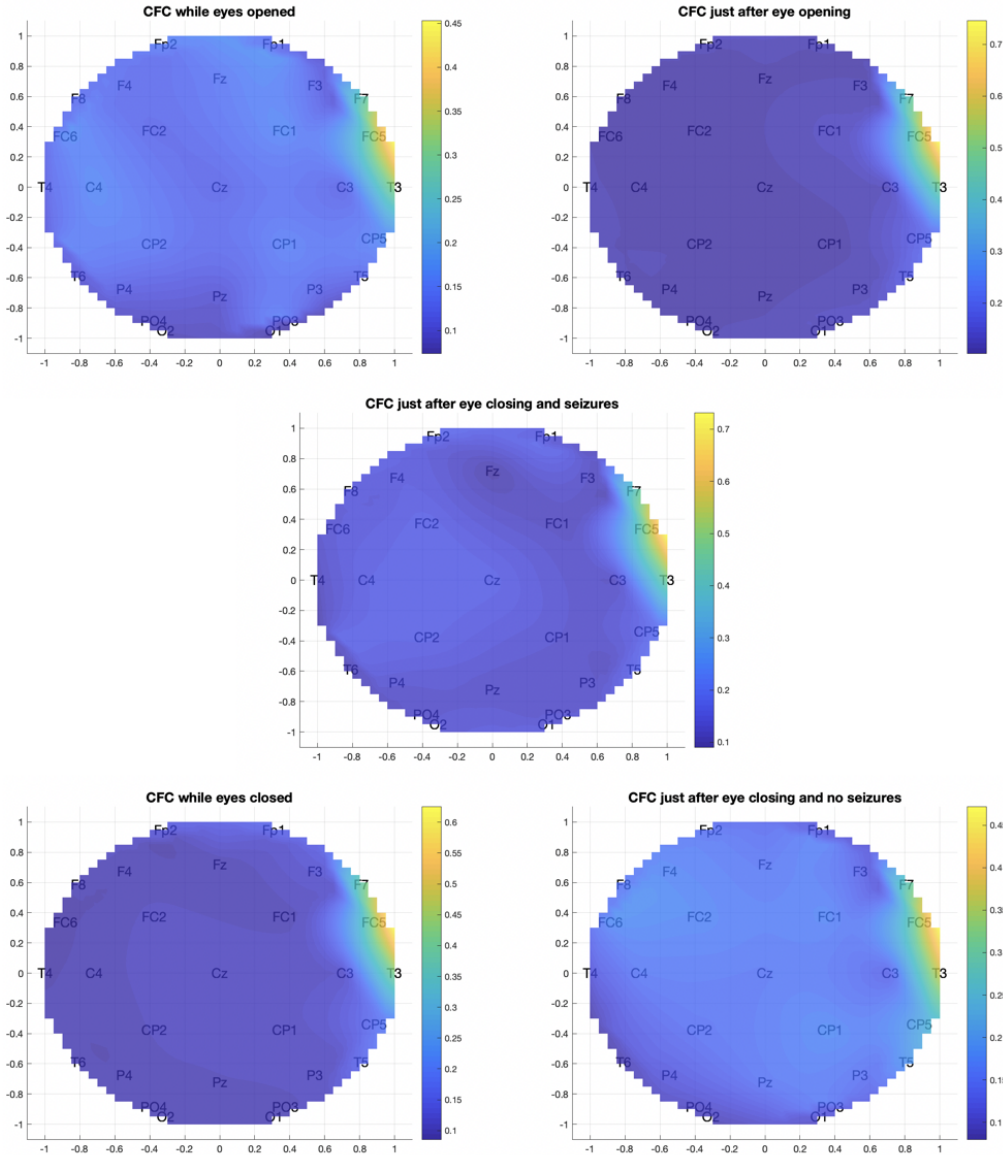


Figure 5.13. Representation of the heatmap to illustrate the PAC of the coupling between alpha and gamma rhythms divided in the five cases of clinical interest

Going to analyse the coupling between alpha and gamma rhythm, a strong coupling in the temporal-frontal area can be seen. Note the values that are reached in the case of eye closure and a seizure immediately afterwards.

PAC index for theta-beta rhythm

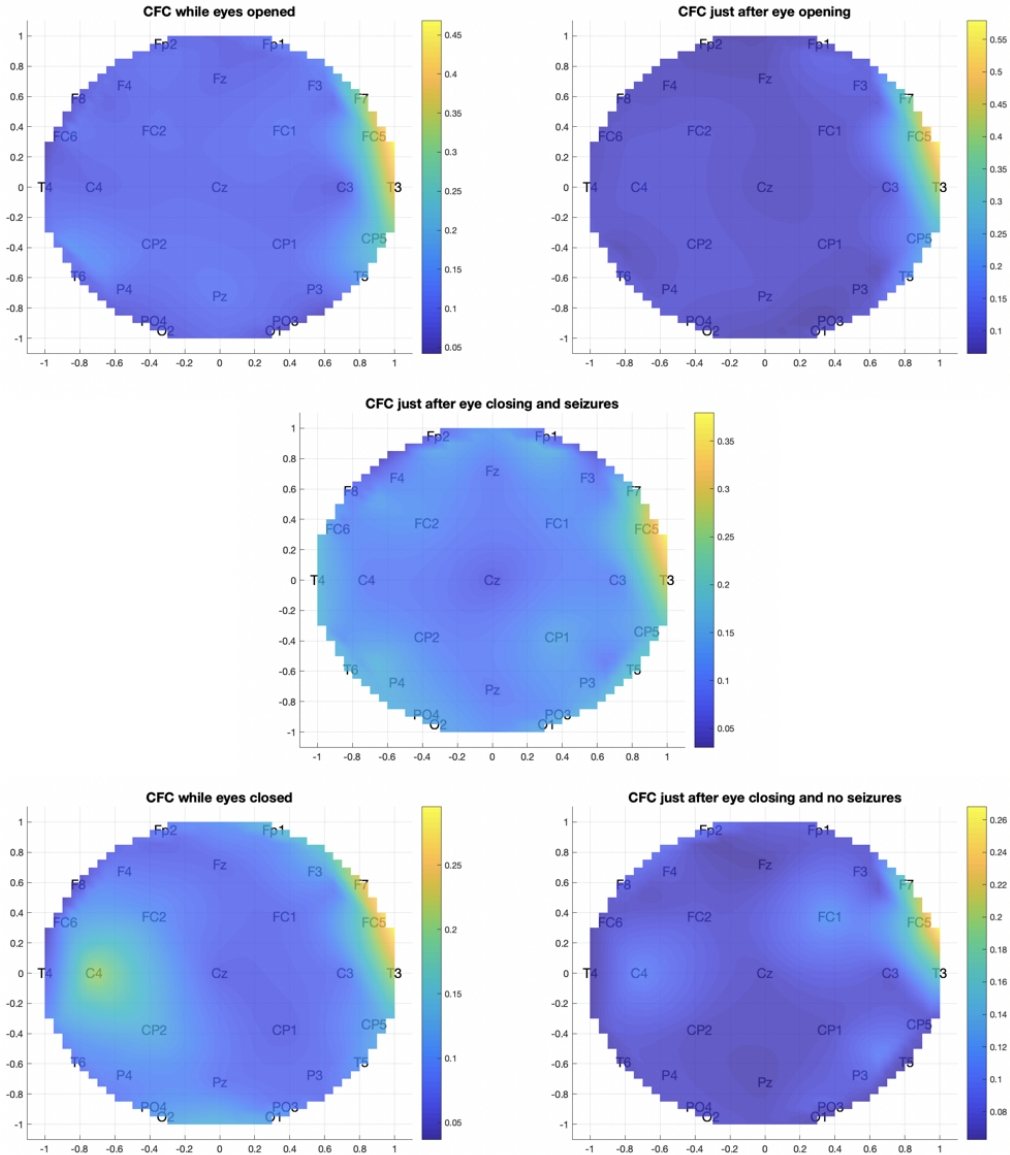


Figure 5.14. Representation of the heatmap to illustrate the PAC of the coupling between theta and beta rhythms divided in the five cases of clinical interest

Also for this frequency couple a higher level at the height of the temporal-frontal region is noted, but compared to the previous case, lower index values are reached.

Chapter 6

Conclusion

After having elaborated all of the individual patient tracks and analysed for each of them the indexes and related cases shown above, I wondered if there was an analogy between them. We have seen that among the results obtained there are some characteristics that recur within the same patient but it is difficult to notice some of them among various patients.

At the end of my study, we asked ourselves how we could continue this work in the future in order to continue to obtain new information from the study of the EEG signal.

At the basis of everything that concerns ourselves there is a dense and complex network of nervous communication controlled exclusively by the brain. How this organ functions and how its different regions communicate with each other remains one of the most studied questions in the field of neuroscience.

Among the most discussed topics in recent years is the report between neurophysiological processes, consciousness and brain functions such as attention, perception, memory and language. Understanding the relationship between brain structure and function is one of the fundamental questions of neuroscience.

In order to have a more complete perspective of what is happening at the brain level, it is necessary to take into account not only local and global structural changes but also the way these different aspects are related.

6.1 Future Work

In this thesis work for the study of cross-frequency coupling, we focused on the study of coupling between different frequency bands that make up the EEG signal, going to study the results separately for each of them.

A subsequent work could certainly be to examine coupling between other frequency bands, particularly interesting would be the study of theta-gamma coupling. Another consideration about our study is the fact that not all possible electrode

pairs were compared, but only couplings between the occipital electrodes and the others. Therefore one electrode always remained one of the electrodes placed on the occipital lobe while the other channel compared varied from time to time.

So also in this case, it will certainly be interesting to go into this aspect in depth, that is to go and analyse different pairs of electrodes.

Once we have examined the different brain rhythms and studied their coupling between different recording channels, the next step could be the study of functional connectivity. Briefly, functional connectivity is the study of the synchronization strength of neuronal activity in different regions of the brain.

The various techniques and methods developed for the study of brain activity have shown that the different neuronal regions of the brain do not operate in isolation but interact with each other forming a complex network of connections. The study of the relationships/connections existing between the different cortical regions is commonly referred to as the study of brain connectivity.

The functional information usually used for connectivity estimation is provided through non-invasive imaging techniques, based on hemodynamic measurements e.g. functional magnetic resonance imaging, fMRI, metabolic, with the position emission tomography, PET, electrical, such as electroencephalography, EEG, or electromagnetic, through magnetoencephalography, MEG.

6.1.1 Functional Connectivity

As defined in 1994 by Professor Friston, functional connectivity is defined as the temporal coincidence of spatially distant neurophysiological events. The assumption behind this technique is that the similarity in temporal trends of signal fluctuations in different areas suggests that they are in constant communication forming a functional network. Several studies have analyzed the coherence of these networks, showing it under physiological conditions. Neurophysiologic coherence among different locations varies under pathological conditions. [37]

In order to proceed with the analysis of functional connectivity, reference is made only to statistical dependencies among the measured data and no knowledge or assumptions regarding the structure and mechanisms of the neural system are included. An important point to underline is that what is of interest in the end is not the study of functional connectivity point by point but the information that can be deduced from the patterns of related activities.

Numerous methodologies exist to study functional connectivity, as shown in Figure 6.1.

The methods are mainly divided into two categories: frequency-based and time-series-based. The first subgroup is subsequently composed of the coherence analysis and the study of the transfer function. [38]

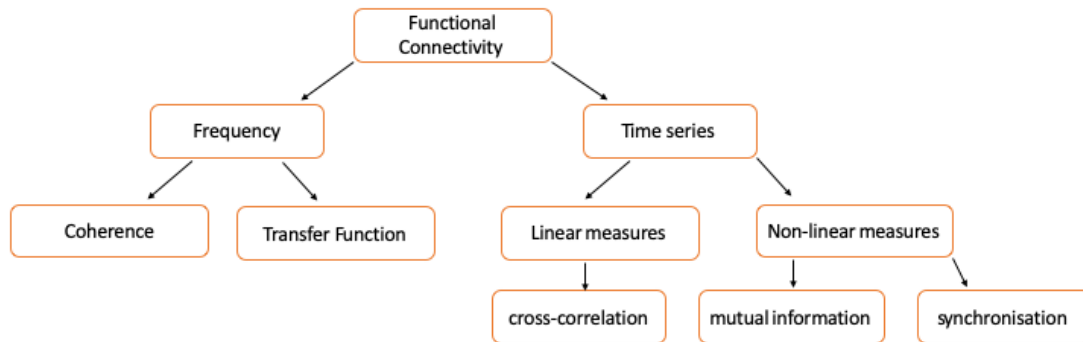


Figure 6.1. *Overview of the main functional connectivity survey groups.*

Those based on time-series provide a further subdivision between linear and non-linear measurements, i.e. a subdivision between hypotheses of gaussianity and non gaussianity of data. In the first case the cross-correlation between time series is analysed, while in the second case the mutual information or synchronisation is evaluated.

Among the most widely used methods for the study of functional connectivity in non-Gaussian time series, there are certainly ICA and PCA analysis.

A disadvantage in the calculation of functional connectivity is that we do not know unambiguously the correlation between different areas. Considering for example two temporal series x and y , coming from two different functionally correlated brain regions, it is not possible to establish univocally if:

- it is x to influence y
- it is y to influence x
- the two areas condition each other
- both are modulated by a third variable

In summary, the brain can be schematised as a brain network composed of nodes and links: the nodes represent the regions of the brain and the links are the connections. Functional connectivity aims to establish the type of connection that binds each node. To do this, the time series that define the brain activity of a certain area are extracted and studied in function of the others.

References

- [1] R. Nieuwenhuys, J. D. Voogd, and C. V. Huijzen, “Il sistema nervoso centrale,” *Springer Science and Business Media*, 2010.
- [2] Mesin, “Introduction to biomedical signal processing,” *Brossura*, vol. 134, pp. 223–244, 09 2017.
- [3] L. Muñoz, R. D. Pinzon Morales, and G. Castellanos-Dominguez in *EEG Rhythm Extraction Based on Relevance Analysis and Customized Wavelet Transform*, vol. 9107, pp. 419–428, 06 2015.
- [4] P. F. Diez, V. Mut, E. Laciari, and E. Avila, “A comparison of monopolar and bipolar eeg recordings for ssvep detection,” pp. 5803–5806, 2010.
- [5] M. E. Avanzolini G., “Strumentazione biomedica. progetto e impiego dei sistemi di misura,” *Patron*, 2015.
- [6] P. C. Lauterbur, “Image Formation by Induced Local Interactions: Examples Employing Nuclear Magnetic Resonance,” vol. 242, pp. 190–191, Mar. 1973.
- [7] B. B. Biswal, J. V. Kylene, and J. S. Hyde, “Simultaneous assessment of flow and bold signals in resting-state functional connectivity maps,” *NMR in Biomedicine*, vol. 10, no. 4-5, pp. 165–170, 1997.
- [8] M. T, L. M, C. DW, F. P, and L. L, “Electrophysiological Correlates of the BOLD Signal for EEG-Informed fMRI,” *Human Brain Mapping*, vol. 36, pp. 391–414, 2015.
- [9] H. Laufs, “A personalized history of eeg–fmri integration,” *Neuroimage*, vol. 62, no. 2, pp. 1056–1067, 2012.
- [10] J. W. Sander, “The epidemiology of epilepsy revisited,” *Current opinion in neurology*, vol. 16, no. 2, pp. 165–170, 2003.
- [11] I. E. Scheffer, S. Berkovic, G. Capovilla, M. B. Connolly, J. French, L. Guilhoto, E. Hirsch, S. Jain, G. W. Mathern, S. L. Moshé, *et al.*, “Ilae classification of the epilepsies: position paper of the ilae commission for classification and terminology,” *Epilepsia*, vol. 58, no. 4, pp. 512–521, 2017.
- [12] X. Jiang, G.-B. Bian, and Z. Tian, “Removal of artifacts from eeg signals: A review,” *Sensors*, vol. 19, p. 987, Feb 2019.
- [13] J. Valderrama, A. Torre, and B. Van Dun, “An automatic algorithm for blink-artifact suppression based on iterative template matching: Application to single channel recording of cortical auditory evoked potentials,” *Journal of Neural*

- Engineering*, vol. Accepted, 09 2017.
- [14] H. Jung, Makeig, “Removing electroencephalographic artifacts by blind source separation,” *Psychophysiology*, vol. 37, no. 2, pp. 163–178, 2000.
 - [15] A. Q. Hamal and A. W. b. A. Rehman, “Artifact processing of epileptic eeg signals: An overview of different types of artifacts,” pp. 358–361, 2013.
 - [16] K. J. Lee, C. Park, and B. Lee, “Elimination of eeg artifacts from a single-channel eeg using sparse derivative method,” pp. 2384–2389, 2015.
 - [17] A. S. s. Mandli Rami Reddy, Ravi Chandra, “A fast adaptive speech extraction method using blind source separation for audio signal processing,” *Blue Eyes Intelligence Engineering and Sciences Publication*, vol. 9, 02 2020.
 - [18] A. Hyvärinen and E. Oja, “Independent component analysis: algorithms and applications,” *Neural networks*, vol. 13, no. 4-5, pp. 411–430, 2000.
 - [19] P. J. Huber, “Projection pursuit,” *The annals of Statistics*, pp. 435–475, 1985.
 - [20] C. P, “Independent component analysis — a new concept?,” *Signal Processings*, vol. 34, pp. 287–314, 1994.
 - [21] M. S, J. TP, B. AJ, G. D, and S. TJ, “Blind separation of auditory event-related brain responses into independent components,” *Proceedings of the National Academy of Sciences of the United States of America*, vol. 37, pp. 10979–10984, 10 1997.
 - [22] T.-P. Jung, S. Makeig, M. Westerfield, J. Townsend, E. Courchesne, and T. Sejnowski, “Analyzing and visualizing single-trial event-related potentials,” *Advances in Neural Information Processing Systems*, vol. 11, 09 2000.
 - [23] A. Delorme and S. Makeig, “Eeglab: an open source toolbox for analysis of single-trial eeg dynamics,” *Journal of Neuroscience Methods*, vol. 134, pp. 9–12, 01 2004.
 - [24] A. Bell and T. Sejnowski, “An information-maximization approach to blind separation and blind deconvolution,” *Neural computation*, vol. 7, pp. 1129–59, 12 1995.
 - [25] V. Zarzoso and P. Comon, “Robust independent component analysis by iterative maximization of the kurtosis contrast with algebraic optimal step size,” *IEEE Transactions on Neural Networks*, vol. 21, p. 248–261, Feb 2010.
 - [26] T. T. Munia and S. Aviyente, “Time-frequency based phase-amplitude coupling measure for neuronal oscillations,” *Scientific reports*, vol. 9, no. 1, pp. 1–15, 2019.
 - [27] J. E. Lisman and O. Jensen, “The theta-gamma neural code,” *Neuron*, vol. 77, no. 6, pp. 1002–1016, 2013.
 - [28] M. J. Hülsemann, E. Naumann, and B. Rasch, “Quantification of phase-amplitude coupling in neuronal oscillations: Comparison of phase-locking value, mean vector length, modulation index, and generalized linear modeling cross-frequency coupling,” *Frontiers in neuroscience*, vol. 13, p. 573, 2019.
 - [29] A. B. Tort, R. Komorowski, H. Eichenbaum, and N. Kopell, “Measuring

- phase-amplitude coupling between neuronal oscillations of different frequencies,” *Journal of neurophysiology*, vol. 104, no. 2, pp. 1195–1210, 2010.
- [30] R. T. Canolty, E. Edwards, S. S. Dalal, M. Soltani, S. S. Nagarajan, H. E. Kirsch, M. S. Berger, N. M. Barbaro, and R. T. Knight, “High gamma power is phase-locked to theta oscillations in human neocortex,” *science*, vol. 313, no. 5793, pp. 1626–1628, 2006.
- [31] Y. Salimpour and W. S. Anderson, “Cross-frequency coupling based neuromodulation for treating neurological disorders,” *Frontiers in neuroscience*, vol. 13, p. 125, 2019.
- [32] U. J. Chaudhary, R. Rodionov, D. W. Carmichael, R. C. Thornton, J. S. Duncan, and L. Lemieux, “Improving the sensitivity of eeg-fmri studies of epileptic activity by modelling eye blinks, swallowing and other video-eeg detected physiological confounds,” *Neuroimage*, vol. 61, no. 4, pp. 1383–1393, 2012.
- [33] A. E. Vaudano, A. Ruggieri, M. Tondelli, P. Avanzini, F. Benuzzi, G. Gessaroli, G. Cantalupo, M. Mastrangelo, A. Vignoli, C. D. Bonaventura, *et al.*, “The visual system in eyelid myoclonia with absences,” *Annals of neurology*, vol. 76, no. 3, pp. 412–427, 2014.
- [34] P. Jeavons, “Nosological problems of myoclonic epilepsies in childhood and adolescence,” *Developmental Medicine & Child Neurology*, vol. 19, no. 1, pp. 3–8, 1977.
- [35] G. Gómez-Herrero, W. De Clercq, H. Anwar, O. Kara, K. Egiazarian, S. Van Huffel, and W. Van Paesschen, “Automatic removal of ocular artifacts in the eeg without an eeg reference channel,” in *Proceedings of the 7th Nordic Signal Processing Symposium-NORSIG 2006*, pp. 130–133, IEEE, 2006.
- [36] G. Gomez-Herrero, W. De Clercq, H. Anwar, O. Kara, K. Egiazarian, S. Van Huffel, and W. Van Paesschen, “Automatic removal of ocular artifacts in the eeg without an eeg reference channel,” pp. 130–133, 2006.
- [37] K. Friston, C. Frith, P. Liddle, and R. Frackowiak, “Functional connectivity: the principal-component analysis of large (pet) data sets,” *Journal of Cerebral Blood Flow & Metabolism*, vol. 13, no. 1, pp. 5–14, 1993.
- [38] K. E. Stephan, “On the role of general system theory for functional neuroimaging,” *Journal of anatomy*, vol. 205, no. 6, pp. 443–470, 2004.